UNIVERSIDADE DE LISBOA

FACULDADE DE CIÊNCIAS

DEPARTAMENTO DE BIOLOGIA ANIMAL

**Ciências ULisboa**

# Analysis of the breathing apparatus of the cerambycid species that colonizes pines infected by the pine wood nematode, *Bursaphelenchus xylophilus* (Steiner and Buhrer, 1934) Nickle, 1970, with special emphasis to the insect-vector *Monochamus galloprovincialis* (Olivier, 1795).

Ana Catarina Guerreiro Leal

**Mestrado em Ecologia e Gestão Ambiental**

Dissertação orientada por:
Professora Maria Teresa Rebelo (FCUL)
Professor Manuel Francisco Pereira (IST)

2020

## Agradecimentos

**Resumo**

A Doença da Murchidão do Pinheiro foi primeiramente detetada em Portugal em 1999 na Marateca, Península de Setúbal. O agente causador desta doença, que leva à morte da árvore infetada, é *Bursaphelenchus xylophilus*, um nematode micofágico, oriundo da América do Norte, que coloniza várias espécies de coníferas, especificamente *Pinus* spp, usando como vetor um inseto do Género *Monochamus* (Coleoptera).

Enquanto que as espécies nativas da América apresentam resistência, ou alguma tolerância à infeção por parte do nematode, as espécies Asiáticas e Europeias são suscetíveis, desenvolvendo uma sintomatologia característica, que leva ao rápido apodrecimento e morte da árvore. Este facto suporta a teoria de que o Nematode da Madeira do Pinheiro (como ficou conhecido) terá sido transportado desde a América até ao Japão, onde a doença foi inicialmente detetada no início do século XX, em madeira infetada e não tratada.

Após a entrada no Japão, o nematode espalhou-se rapidamente pela China, Tailândia e Coreia. A doença é o resultado de uma complexa interação entre o nematode, o inseto-vetor, a conífera hospedeira e vários fatores climáticos, o que atrasou a atribuição de uma relação causa-efeito entre a presença do nematode e os sintomas da doença, permitindo a larga propagação da mesma.

Em Portugal, e na Europa, tem afetado essencialmente espécies como *Pinus nigra*, *P. sylvestris* e *P. pinaster*, representado perdas significativas de rendimentos e de biodiversidade. Devido ao seu grande potencial destrutivo, o Nematode de Madeira do Pinheiro (NMP) está listado na Diretiva Europeia 2000/29/CE para medidas de proteção contra a introdução e propagação de organismos prejudiciais o que levou a restrições na comercialização de madeiras e de subprodutos não tratados tal como de plantas vivas.

O nematode, que mede apenas 1.5 milímetros, tem uma alta taxa de reprodução e um ciclo de vida de duas fases, uma em que se alimenta de fungos e outra em que se alimenta de células vivas do parênquima. Também se desenvolve de duas formas distintas; se as condições forem favoráveis desenvolve-se rapidamente sob a forma "Reprodutora", se as condições começarem a ser desfavoráveis, ou seja, quando a árvore hospedeira decai, desenvolve-se como uma forma de "Dispersão" que é uma forma mais resistente. É nesta fase que o nematode migra para junto das câmaras pupais do inseto vetor e aguarda pela muda das pupas para infestar os adultos recém-formados.

O inseto vetor do Género *Monochamus* com distribuição em Portugal é *M. galloprovincialis* (Olivier,1795), um besouro endémico Cerambicídeo, da subfamília Lamiinae, considerado uma praga secundária pelo que não existia muita informação sobre a sua ecologia e anatomia antes da entrada do nematode no país. Tem um ciclo de vida univoltino ou seja, produz descendência apenas uma vez no ano, para se reproduzir tem de se alimentar de rebentos da copa de pinheiros saudáveis, a chamada alimentação de maturação sexual. Os machos produzem feromonas para atrair as fêmeas para a reprodução e as fêmeas para ovipositar necessitam de pinheiros em declínio ou mortos recentemente.

As larvas e pupas do inseto vetor, e outros colonizadores dos pinheiros, convivem com juvenis do nematode dentro da madeira do pinheiro durante os vários meses de desenvolvimento do inseto. De alguma forma, o nematode identifica as pupas do inseto vetor e aguarda pela última muda para entrar no sistema respiratório através dos espiráculos dos adultos recém-formados.

O inseto depois emerge da árvore hospedeira, transportando o nematode e transmitindo-o para novas árvores durante a sua alimentação, ocorrendo a "Transmissão Primária". As fêmeas infetadas, quando depositam os seus ovos em árvores enfraquecidas também podem transmitir o nematode, ocorrendo a chamada "Transmissão Secundária".

Inserido no Projeto NEMATRANSFER (PTDC/AGR-FOR/4391/2014), esta dissertação visa a análise do Sistema Respiratório, espiráculos e traqueia, do inseto vetor e de 3 outras espécies colonizadoras do pinheiro bravo, nomeadamente *Arhopalus syriacus* (Reitter, 1895), *Acanthocinus griseus* (Fabricius, 1793), e *Pogonocherus perroudi* Mulsant, 1839 que são as mais abundantes e mais próximas filogeneticamente da espécie vetora, na tentativa de isolar características que possam ser barreiras físicas à entrada do nematode nas espécies não vetores, na expectativa que os dados obtidos possam ser usados na criação de novas medidas de gestão de pragas. Para alcançar o objetivo principal, foram testados protocolos de preparação de exemplares para se conseguir uma caracterização dos espiráculos (tamanho e existência, ou não, de sedas) através de imagens obtidas em Microscopia Eletrónica de Varrimento (MEV) e medições da traqueia e suas ramificações usando Micro Tomografia de raio X (Micro-CT) e modelos 3D dos exemplares.

A Micro-CT é uma técnica não invasiva, baseada na interação dos raios X com os diferentes constituintes da amostra, que permite a observação da anatomia interna dos exemplares uma vez que produz imagens de alta resolução que podem depois ser integradas para gerar um volume virtual da mesma. Esta técnica permite também individualizar partes dos exemplares, por exemplo certos órgãos, usando o *software* CTAnalyzer (distribuído por BRUKER®), também conhecido como "Segmentação".

A MEV é amplamente usada para observar estruturas ao nível da superfície das amostras. Um feixe de eletrões, chamados eletrões primários, passa rapidamente pela superfície da amostra. Antes da observação em MEV, a mostra é metalizada com ouro, ou ouro-paládio, para promover a emissão de eletrões, chamados eletrões secundários, o impulso elétrico é depois detetado e transformado numa imagem.

Para a preparação e estabilização dos exemplares para suportarem estas técnicas, tentou-se a Fixação Química com glutaraldeído e tetróxido de ósmio seguida de Secagem pelo método do Ponto Crítico e como alternativa a este processo moroso, a Liofilização que consiste numa sublimação a baixa pressão e temperatura. Obtivemos sucesso em ambos os procedimentos, com percentagens semelhantes entres estes, no entanto não foi possível preparar o mesmo número de indivíduos com ambas as técnicas, pois as larvas recolhidas não eram igualmente distribuídas pelas quatro espécies em análise e algumas larvas morreram antes da muda. Os exemplares estabilizados foram observados no microscópio eletrónico para avaliar a sua integridade e foram distribuídos entre as técnicas de observação, MEV ou Micro-CT.

Devido ao moroso processo de estabilização e ao tempo gasto na resolução dos problemas metodológicos e na agilização do processo de tratamento dos exemplares, não foi possível atingir as repetições inicialmente planeadas e necessárias para uma avaliação estatística adequada sobre o sucesso entre os diferentes métodos de preparação.

As fotografias dos espiráculos, obtidas na MEV, foram analisadas com o *software* ImageJ e as medições obtidas foram trabalhadas em Excel. Foi medida a área total de 199 espiráculos de 1 pupa e 9 adultos *M. galloprovincialis*, 2 pupas e 10 adultos *A. Syriacus*, 3 *A. griseus* adultos e *1 P. perroudi*. tal como a área do espiráculo não coberta por sedas e a circularidade, uma razão entre a área e o perímetro, automaticamente calculada pelo ImageJ, que permite classificar a forma do espiráculo como mais circular, se o valor se aproximar de 1, ou mais elíptica se o valor se aproximar de 0.

Os resultados obtidos através das medições feitas, indicam que os espiráculos dos adultos de *M. galloprovincialis* são os que apresentam a menor percentagem de área descoberta, ou seja, a área em que não há sedas a cobrir a entrada do espiráculo, quando comparados com os adultos das outras três espécies estudadas, que não desempenham um papel de disseminação do nematode. Enquanto que os espiráculos dos adultos das espécies *A. syriacus* e *A. griseus* estão mais desprotegidos, tendo uma menor percentagem de cobertura de sedas, os espiráculos de *M. galloprovincialis* têm mais sedas que poderão ser facilitadoras do movimento do nematode para dentro do espiráculo enquanto também preservam um nível de humidade favorável à sobrevivência, e à própria movimentação, do NMP. Por outo lado, as

pupas de *M. galloprovincialis* apresentam uma cobertura de sedas ainda maior que o adulto da mesma espécie, o que nesta fase de desenvolvimento do inseto pode atuar como uma barreira física à entrada do nematode e que poderá explicar por que razão este só infecta o inseto adulto.

Apesar de várias dificuldades em agilizar o processo de segmentação que acabou por inviabilizar a individualização da rede de ramificações da traqueia, através das radiografias obtidas da Micro-CT foi possível identificar quatro principais ramificações na cabeça e tórax e duas ramificações no abdómen de insetos das espécies *M. galloprovincialis*, *A. syriacus* e *A. griseus,* que são consistentes com as descrições morfológicas consultadas. Também foi possível medir o diâmetro das ramificações, nesses mesmos indivíduos, e posteriormente fez-se uma estimativa do volume das traqueias observadas. Os resultados obtidos das medições, indicam que o volume total da traqueia é maior em insetos maiores, o que corrobora o fato de as traqueias se estenderem por todo o corpo para que o oxigénio chegue a todos os órgãos e tecidos. Ao comparar o macho e a fêmea de *M. galloprovincialis* é notável a diferença de volume da traqueia ao nível do abdómen, sendo o da fêmea praticamente o dobro do macho, mas o volume total de ambos é semelhante o que sugere que poderá haver uma distribuição desigual das ramificações da traqueia consoante o sexo, para esta espécie, o que não se verifica no macho e fêmea de *A. griseus* que foram também medidos.

Todos estes pontos resultantes do trabalho feito e da comparação entre a espécie vetor do NMP e as outras espécies estudadas, que convivendo com o nematode nas árvores hospedeiras não desempenham um papel de disseminadoras, poderão trazer novas perspetivas sobre a complexa interação entre o inseto vetor e o NMP. Todo o trabalho feito na preparação dos indivíduos é também uma mais valia para futuros trabalhos que tenham como objetivos a observação de estruturas anatómicas semelhantes. Todos os dados obtidos são originais e podem ser relevantes para futuras propostas de gestão do NMP

**Palavras chave:** Gestão Integrada de Pragas, Nematode da Madeira do Pinheiro, Cerambicídeo, Micro Tomografia, Microscopia Eletrónica de Varrimento

**Abstract**

The Pine Wilt Disease (PWD) is caused by a non-indigenous nematode, *Bursaphelenchus xylophulis,* that disseminates widely through a flying insect-vector, *Monochamus galloprovincialis* (Oliver, 1795), colonizer of the pine tree, leading the trees to death due to the clogging of the tree vessels. It remains unknown how the nematode identifies and infect the newly formed adult individuals of the vector species. Whereby, in the procedure of the project NEMATRANSFER (PTDC/AGR-FOR/4391/2014), we compare anatomic structures of pupae and adult insects of the vector species and other three cerambycid species, *Arhopalus syriacus* (Reitter, 1895), *Acanthocinus griseus* (Fabricius, 1793), and *Pogonocherus perroudi* Mulsant, 1839, in as attempt to recognize differences that may be considered as physiological barriers to nematode entry in non-vector species.

To accomplish the main goal, several protocols were tried to achieve a characterization of the spiracles (measures, existence, or not, of bristles) using Scanning Electron Microscopy images and to measure the tracheal system (its length, ramifications, etc.) with Micro-computed Tomography and 3D models using proper software.

From the obtained SEM results we presume that, while the non-vector species spiracles', have lower bristles coverage, the insect-vector has only a small area not covered by them. This can imply that the bristles should help the nematode to tangle itself and crawl into the trachea while provide a moisture environment that also favour the nematode survival and movement. On the other hand, the bristles coverage of the pupae may be so dense that in this stage of the insect development it can work like an obstacle for the nematode entrance. This may be the reason why the PWN enter the spiracles only when the newly adult insects are formed. It has found evidence that the shape of the spiracles may represent an important feature to explain how PWN colonizes the insect-vector, or why it prefers *M. galloprovincialis* over the other species.

In what concerns the Micro-CT results, we were able to identify four main tracheal trunks in the head and thorax and two main trunks in the abdomen of *M. galloprovincialis*, *A. syriacus* and *A. griseus* specimens. Also it was possible to measure tracheal trunks in one lyophilized specimen, in specimens fixated with glutaraldehyde and osmium tetroxide, and critical point dried, and even in not treated specimens, although in this last case it was harder to find the main trachea trunks lengthwise the entire body of the insect. The volume estimated values obtained are consistent with the insects' body length, being higher in bigger specimens, and diameter and number of the main trunks are consistent with the described morphology of the trachea ramifications for Coleoptera insects. By comparing the abdominal tracheal volumes of both *M. galloprovincialis* male and female specimens, it seems that a differential ramification arrange occurs, as the female abdominal tracheal volume is twice of the male while the total volume is similar.

All the worked done for the stabilization and preparation of the samples to endure SEM and Micro-CT is an asset for future similar studies. Our results, obtained by comparing the vector species with the non-vector species, that also share the host tree but do not have a role in the spread of the nematode may bring some understanding about the complex interaction between the PWN and the insect- vector. All our data are original and may be relevant for future pest managements measures.

**Keywords:** Pest management, Pine Wood Nematode, Cerambycid, Micro-CT, Scanning Electronic Microscopy.

# Index

**List of Figures**

**List of Tables**

# 1    Introduction

Pine Wilt Disease (PWD) is an illness affecting pine trees, which is caused by the pinewood nematode *Bursaphelenchus xylophilus* (Steiner and Buhrer, 1934) Nickle, 1970 [1]. It results from a complex interaction between a nematode, its flying insect-vector (a *Monochamus* spp., colonizer of the pine tree) and the host tree, leading to the death of pine trees due to the clogging of the conducting vessels [2] being one of the most serious worldwide conifer disease affecting native species of *Pinus* spp. from East Asia to Europe [3].

The pine wood nematode (PWN) is native from North America and colonizes conifers trees, mainly *Pinus* spp. As the dead wood of native species provides the substrate for his development, only a few ones are susceptible to be attacked as living trees [1,2]; the European species, for example, *Pinus nigra*, *P. sylvestris* and *P. pinaster*, are some of the species susceptible to the nematode and known to be killed by the PWD as adult trees, while native American species are mostly resistant, or at least tolerant once they have developed physical or biochemical barriers to prevent direct invasion to healthy tissues. This supports the theory that *B. xylophilus* was transported on infected, untreated timber exported from America to the southern Japanese islands where it was first detected at the first decades of the 20th century [2,4].

Afterwards, it spreads to China, Taiwan and Korea. In Europe, PWD was primary detected in Portugal in 1999 [3], at Marateca in Setúbal Peninsula and it is believed that the point of entrance of PWN was Setúbal seaport through imported non-treated infected wooden pallets or wood packaging, being latter confirmed its presence in Madeira Island and in two foci in Spain in 2010. Since it was first detected in Mediterranean Basin, through multiple surveys and samplings, the nematode is still mainly confirmed to maritime pine, *P. pinaster*.

Data from North America and Japan indicates that maybe not only the species of the host tree determines the mortality due to expression of PWD; factors like tree condition, soil type, moisture content and temperature also have influence on the symptom expression [5]. In fact, there was lack of research to assess the impact of the factors mentioned above in the arising mortality from expression of PWD. More complex still, is the interaction between the nematode and its insect vector, subject that has been studied by scientist from the countries facing this problematic forest pest.

Those factors and the fact that the only common organism in whatever area the disease is register is the nematode, while the species of the host tree and the species of the insect vector varies geographically, are some of the reasons why it took several years to diagnose all the symptoms and to assign a cause effect relation between the presence of the nematode and the PWD. On the other hand, the intensification of international trades and commercialization of infected wood and wood products, are the probable cause of the current broad geographical distribution of *B. xylophilus* and its abnormal killing in the regions newly infected, representing an immediate threat to pine ecosystems all over Europe [6] and an obstacle for a successful eradication [3] thus resulting in a high risk of international spread.

PWD became one of the most worldwide damaging forest pests, reason why is listed as a quarantine organism; in Japan has caused until today, remarkable loses of pine trees (*P. densiflora, P. thunbergii and P. luchuensis*) [1] with annual losses of about 26 million cubic meters (m$^3$) of timber since 1954, representing significant economic and environmental damages, increased cost in management procedures and irreversible changes to the native ecosystems, including loss of biodiversity and wildlife habitat destruction once the main control measure is the cut of wilt trees [3].

The Mediterranean Basin, and Portugal itself, presents a high risk to PWD due to favourable environments with long periods of hot and dry climatic conditions, the existence of forest with the susceptible species already mentioned and the presence of multiple potential vectors of *Monochamus* genus and others which have similar biological and ecology features [6] and despite the efforts of the Portuguese National Forestry (ICNF) and Quarantine Authorities (DGAV), the disease has spread to new forest areas [3].

In Portugal, the insect vector for the PWN is the pine sawyer, *Monochamus galloprovincialis* (Olivier, 1795) a longhorn beetle which distribution goes from Central, West and North Europe to Russia, Turkey and Ukraine [1]. It is a flying cerambycid insect characterized by its long pair of antennae and its capacity to produce and detect pheromones. *Monochamus* adult insects feeds on the thin bark of the branches and upper trunk of healthy pines and during this process occurs the transmission of the PWN from the insect to the pine host. As other cerambycids, they are not capable of laying their eggs in healthy pine trees. Therefore, the females, to complete the reproduction, need to find weakened trees [7] to lay their eggs on; then, while oviposition, occurs a secondary infestation by PWN [2,8].

The PWN recognizes *M. galloprovincialis* newly formed adults within the host tree, before adults emerge from it, finding an entrance to the insect body throughout their spiracles [4] being transport in its trachea (respiratory system) and elytra (wing cases) [3]. For the insect, this interaction does not appear to represent any significant decrease in its performance, being able to continue their normal life cycle. However, for the nematode once it causes the death of the host tree, he needs to be transport out of the dying tree into a new one to continue to reproduce. While a tree weakened by fire or other insects may recover and live for more years, the pine trees infected with PWN rapidly ceased the production of oleoresin, weaken and die within a year [3].

According with the Portuguese 6th National Forest Inventory, in the existent 35% of forest soil, *P. pinaster* is the 3rd species with a larger forest area, about 714 thousand hectares (23%), however, the area occupied by resinous species corresponds to 31% of the Portuguese forest [8]. The maritime pine is an important resource due to its economic value; its main products are manufactured wood, pallets, and resin which together represents about 306 million Euros [9]. This helps us to understand the threat that the nematode represents for the forest species, for biodiversity and consequently, for the timber and paper industry to. If the nematode continues to spread, large forest areas are endangered as its biodiversity, with significant economic consequences either by the loss of investments either by the reduction of income [4].

## 1.1    Objectives

Once that it is not known exactly how the nematode identifies the specimens of the vector insect within the pupae chambers in the host tree wood, the main goal is to compare anatomic structures of pupae and adult insects of the vector species and other three cerambycid species, *Arhopalus syriacus* (Reitter, 1895), *Acanthocinus griseus* (Fabricius, 1793), and *Pogonocherus perroudi* Mulsant, 1839, who share geographic distribution and host trees and have similar life cycle features, in an attempt to recognize differences that may be considered as physiological barriers to nematode entry in non-vector species. To achieve the main goal, several protocols will be tried to achieve a characterization of the spiracles (measures, existence, or not, of bristles) using Scanning Electron Microscopy images and to measure the tracheal system (its length, ramifications, etc) with Micro-computed Tomography and 3D models using proper software.

The project NEMATRANSFER (PTDC/AGR-FOR/4391/2014) with those approaches, and complemented by others, such as the analyse and identification of pheromones secreted by the insect vector and of plant volatiles, aims to isolate and understand which factors are used by the nematode to recognise the presence of vector insects and what allows this specific animal to be the carrier of the PWN. It is intended to use the obtained information to improve the current management measures, or ideally tailor integrated pest management measures to fight PWN, and thus break the cycle of infestation and safeguard conifer species.

## 1.2    Pine Wood Nematode

Initially, the designation pine wood nematode was attributed to *Aphelenchoides xylophilus* (Steiner and Buhrer 1934) considered an endemic species to North America and non-pathogenic for native species. Nowadays, Genus *Bursaphelenchus* includes mostly mycophagus (fungal feeders) nematodes, distributed mainly across the Northern hemisphere. Among about 100 species, only two are considered plant parasitic, *B. xylophilus* and *B. cocophilus* the agent of "red ring disease", a serious problem of coconut and palms in Central and South America [3].

The nematode, *Bursaphelenchus lignicolus*, presently known as *B. xylophilus*, was confirmed as the pathogenic agent of PWD in 1971, almost 20 years after the detection of the disease in 1954. Molecular studies carried out on Portuguese populations had established genetic similarities with the Asian populations confirming the origin of its presence in Portugal [9].

*B. xylophilus* is transmitted and spreads through the tree's vascular system and resin canals, has short generation cycles and high reproduction rates (each female can lay between 80 and 150 eggs during an oviposition period of 28 days), it measures only 1,5 millimeter in length and has a two-phase development life cycle, a mycophagous phase in which feeds on fungus and a phytophagous phase (plant or plant tissues feeders) feeding on epithelial cells and living parenchyma cells [10] of axial and radial oleoresin canals and phloem, and also have been found in roots [1].

The nematode develops through two distinct forms, as "reproductive" or "dispersal" life cycles composed of four stages each; the first two stages are common to both, being the first one ($J_1$) completed inside the egg and hatching as the second staged juveniles, $J_2$ [1]. Under favourable conditions (such as suitable temperatures of approximately 20 degree Celsius), the nematodes develop rapidly through the reproductive pathway and moults to the third and fourth juvenile stages ($J_3$ and $J_4$) finally reaching the adult stage as male or female individuals (Figure 1.1) [10] continuing to reproduce.

Primary transmission of PWN to the host tree occurs during summer through the sex maturation feeding of the vector (can see Figure 1.1) when they feed on healthy young pine trees shoots [1] and enters in the host through wounds done in the bark. About 20 to 30 days after infection, as the nematode develops and feed on the tree tissues, the first visible symptoms are abrupt discolouring and wilting of previous-year needles [11]. Then, due to destruction of the epithelial cells of the resin canals, occurs a reduction of oleoresin flow and leaf transpiration ceases and partial interruption in the sapwood obstructs sap flow [9], causing browning of the needles due to water deficiency and the collapse of photosynthesis as a result of blocking the water movement by cavitation of tracheid in xylem of vascular system [10,11]. Later, wilting all over the tree crown and stopping tree's oleoresin flux, ending in an overall rapid decline and dead of the host tree, frequently within a year [3].

While the conditions are favourable, the nematode continues to rapid developing; as the tree decay and environment conditions are not so propitious (like too high or too low moisture levels or absence of food source) the nematode switches to its dispersal pathway, a resistant stage of development [9], being the third and fourth stage juveniles referred as $J_{III}$ and $J_{IV}$ [10]. The last ones surround the pupal chamber, as soon as the callow adult is formed, and enter the insect body to the insect's trachea, through the spiracles and under the elytra, just before the emergence of the adult beetle [1].

One adult beetle flies a maximum distance of 2.5 kilometre and carries around 0.3 million nematodes [10] while the females are looking for suitable trees to oviposit. For that reason, a Secondary Transmission also occurs during oviposition in the bark (see Figure 1.2), but to a lesser extent [9], when females lay eggs on dead or weakened pine trees [4]. The $J_{IV}$ dispersal larva abandon the insect body and enters the host tree through the oviposition wound; the insect is then the dispersive agent of the PWD and cause itself the dead of trees he also needs to reproduce [3].
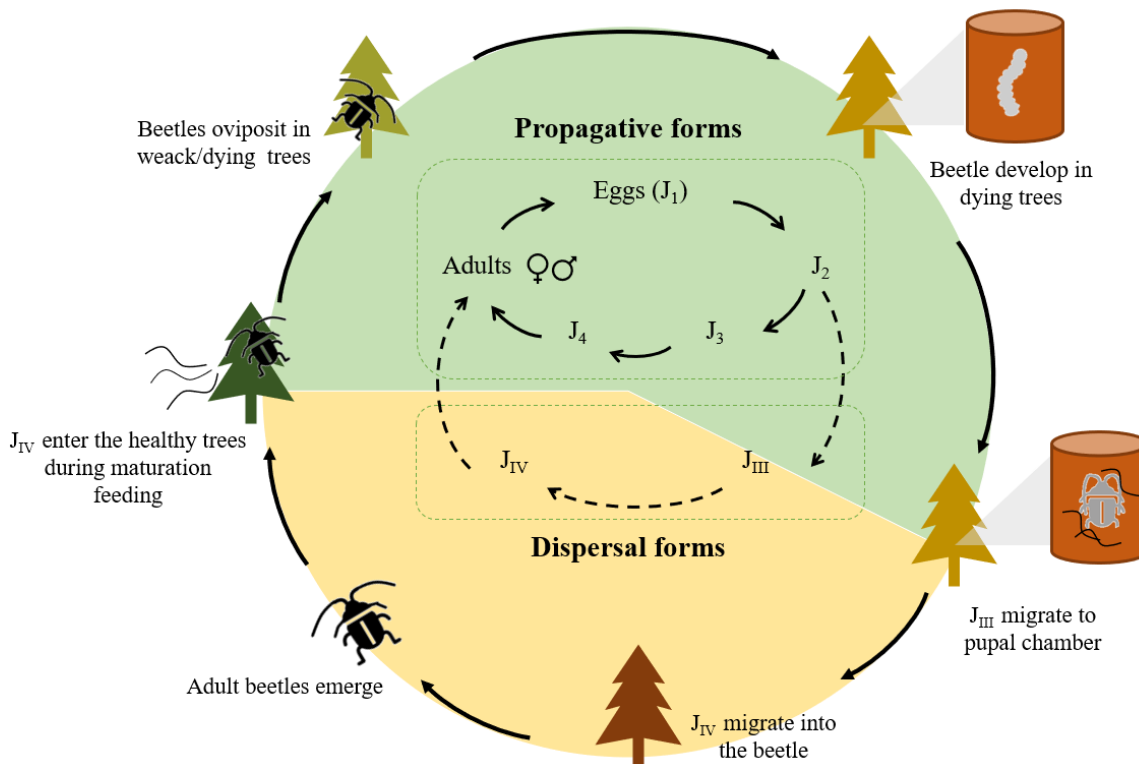


*Figure 1.1: Pine wood nematode life cycle stages and interaction with the insect-vector within the host tree; based on the scheme from reference 10 .*

When detected, the spots affected by the disease were confined to the mainland and the Portuguese national authorities notified the European Commission. Due to their high destructive potential, PWN is listed in Directive No. 2000/29/CE of May 8th concerning protective measures against introduction and spread of harmful organism to plants and plants products in the European Union (EU) and it is also included by the European and Mediterranean Plant Protection Organization (EPPO) as a quarantine organism (EPPPO A2 list) [5]. Therefore, severe restrictions on the movement of plants and trade of untreated pine wood and pine by-products from infected areas were immediately stablished and a Restriction Zone was delimited, including the Affected Zone and a security zone, Buffer Zone at least 20 kilometres around the affected area [4] which has different management measures.

EPPO's recommendations of phytosanitary measures includes prevention of PWN and its vectors, which include that plants and wood of conifers from infested countries should be prohibited or wood products must be treated to a core temperature of 56 degree Celsius for 30 minutes once that heat treatment seems to be the most effective for wood products already infected with PWN [10].

Control measures implemented by EPPO procedures for official control include as well, detection surveys, to be carried annually and be focused on potential points of introduction of *B. xylophilus*, PWD symptoms, and within the time of year when it is likely to develop in the cases where wilt symptoms do not occur, and detection surveys that should be focused on trees and areas with *Monochamus*' signs of activity [5]. To study the insect presence, it can be used multiple funnel trap (that consists of a series of plastic funnels arranged vertically over a collection cup), also a mixture of alpha-pinene, ethanol and methyl-butanol was used as lure but further research on the chemical ecology of the beetle allowed the identification of an aggregation pheromone that is now used in the commercialized lures for insect control [7,10]. Tree vaccination with nematicide, selective breeding of resistant trees, etc. could be more efficient approaches but are extremely expensive and labour rigorous [12]; instead, management of the insect vector has been the "line of attack" to deal with PWN and PWD.

Once in the tree, it is mostly impossible to control PWN, therefore PWD symptomatic and dead trees should be removed as soon as possible; all symptomatic trees are felled outside the flight period of the vector, from the border towards the centre of the infected area and should be cut as close to the soil as possible [5] and then the infected wood is destroyed by burning [9,10]. A minimum area of at least six kilometres radius should be stablished around the infested trees, consisting of 100 -500 meters to three kilometres clear-cut area and an adjacent of at least three kilometres which should be monitored for the presence of the nematode. Clear-cut areas should be kept free from pine trees until B. xylophilus is declared eradicated, these happen when there are no findings of the PWN for, at least, two vector life cycles with a minimum three years of annual monitoring in the area [5].

Despite the implemented control measures, the PWN continued to spread and in 2008 all Portuguese mainland was declared as a Restricted Zone and the Buffer Zone was extended along the border with Spain (Decree-Law No. 99/2011) [5]. The main cause for the rapid dispersion despite the implemented control measures lays in the fact that the symptoms may be often confused with others, caused by biotic or abiotic agents [12], such as bark beetles attack for example, even more, the nematode presence is only confirmed after laboratory observation [9] of samples, and the fact that the symptoms are the result of a complex biological interaction. Therefore, it is of the most urgency to gather knowledge about the environmental factors that play a decisive role in the development of the disease together with anatomy, ecology and physiology features of both nematode and the insect vector, which the last one, is the goal of this work.

## 1.3 The insect-vector

The pine sawyer beetle, *M. galloprovincialis*, is a Coleoptera (Cerambycidae, Lamiinae) which family includes about 20 000 species, in the majority characterized by its elongate body, attractive colors and long antennae, usually at least two-thirds as long as the body length. The number of genera and species found in Europe is very small compared with those found in the Tropics [13]; Genus *Monochamus* includes about 150 species spread across North America, Asia, Europe, where can be found 5 native species, and in Africa where it is particularly numerous [7].

The endemic Portuguese species, *M. galloprovincialis*, found to be the *B. xylophilus* vector, was considered as a rare, secondary forest pest [14]. Beside the descriptions of general Lamiinae features, and the classical paper of Hellrigl from 1971 and the work of Francardi and Pennacchio, both referred in the paper of Naves et. al 2008 [7], its biology and ecology had never been much studied [18]. To develop proper pest management programs to prevent further dissemination of PWD it is necessary detailed knowledge of such subjects.

Lamiinae adult's feed appears necessary for producing offspring, and some feeding usually precedes first copulation in both sexes. For instance, *M. galloprovincialis* feeds on healthy shots for sexual maturation and become sexually mature in 5 to 12 days after emergence and immature males do not release attractants for mature females and immature females are not attracted to mature males [15]. In most species, the eggs are laid in or on the host, in wood fissures, under the bark or bark scales, etc., and larvae phase is long, having the duration of one year, maximum of three years, depending on each species [13].

*M. galloprovincialis* has a univoltine life cycle, which means that has one brood of offspring per year requiring about ten months to develop, although, in colder regions most of the insects require two years to complete their development [18]. To reproduce, females are attracted to stressed, dying or recently dead trees [9] and fresh felled timber, being the pine trees the most important hosts and the eggs laid in slits in the bark [7]. Oviposition period varies from seven to ten weeks [16], eggs develop in one or two weeks during the summer and the newly-hatched larva had a fast development during the warm months in their individual galleries, migrating through the phloem, where they feed.

There is a deficiency of information regarding the number of larval instars in any species of the family Cerambycidae; for *M. galloprovincialis*, Naves et al. 2008 [7] estimated about four or six instars according to head capsule measurements of larva moults. The first stage can last for two or three weeks, as the second stage (or second instar), during which, if larval density is high and intraspecific competition increases, cannibalism can occur, similar with other species of the genera.

As the days grows small by late September, equally to other species of the genera, *M. galloprovincialis* larvae extend their galleries deeply into the wood and most of them are in the third instar [16]. About 40 to 50 days after eggs hatch, larvae can be found in their final instar and as winter become harsh, they overwinter without moulting, which means that they initiate their dormancy period.

Similar larval dormancies have been described for other species, like the Asian *M. alternatus* and *M. saltuarius*; according with the work of Naves, et al. on Winter dormancy of the pine sawyer *M. galloprovincialis* [7] this is an obligatory, genetically induced dormancy associated with pine sawyer's last larval instar. Diapause, that happens at the cold season, apparently regulate the life cycle, prolonging the larval development keeping them safely inside the wood of the host tree and preventing the emergence during the early autumn when the insects could face adverse climatic conditions as an increasing precipitation and a decreasing temperature [4,14].

This period of dormancy can explain the one-year life cycle and the interruption of larval development even at favourable conditions [7]. Even more, the single offspring per year seems to represent an advantage for *M. galloprovincialis* insects as they depend on a very specific and irregular available host trees to be able to breed, which can be an over exploited resource, subject to intense intra and inter-specific competition [14].

After the winter the larvae moult into pupae in their pupal chambers, coated with tiny wood chips of the host tree, where gets through the pupae phase, when it is more vulnerable, lasting for about 20 days [4] (two to three weeks). Initially the pupae have a white colouration, similar to the larvae (see Figure 1.2: A) and a few days before completing their developments, acquire a darker colouration and a harder cuticle stars to form. At the end of the pupae phase (Figure 1.2: D), the newly formed insects emerge from the tree through a perfectly round-shaped hole and flies to find healthy pine trees to feed on new trunks of the crown, necessary for their sexual maturation.
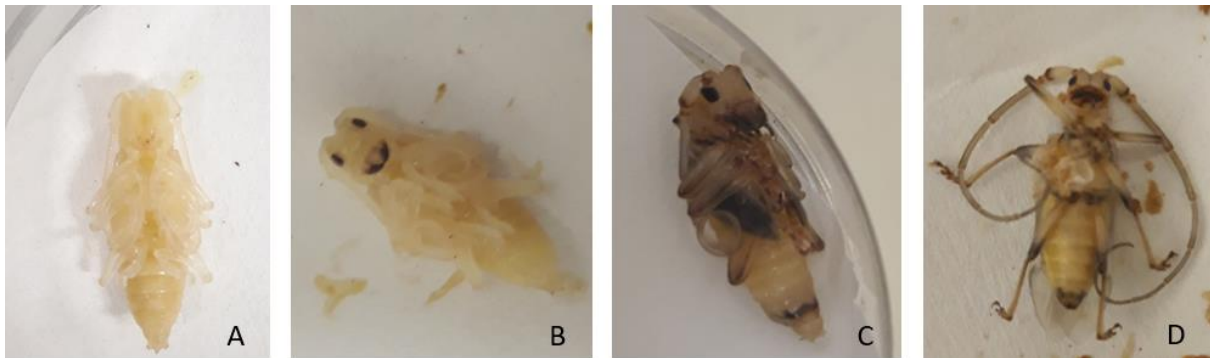


*Figure 1.2: Development of a pupae of M. galloprovincialis: A - recent moulted pupae, B - pupae with about 10 days; C-pupae with his dark coloration, about 15 days after moulting; D - newly formed adult; (Author's original).*

Emergence occurs from May to August [14], or until September with a peak in July as supported by data of the captures of attractive traps [7], and occurs earlier for males than for females. This is a usual trend for the Cerambycidae in general and it is believed that is a reproductive strategy; the males find the oviposition sites, that can be sparse, and they defend it until the emergence of females.

If the tree is already infected, the nematode itself goes through its larvae phases within the wood of the host tree, living for several months among larvae and pupae of different species, including insect vector specimens; but, is only at the final stage of insect pupae phase that the PWN migrates to the pupae chambers parasitizing the newly formed insect-vector adult by finding entrance through the spiracles into the respiratory system. When the adult emerges and during the maturation feeding the nematode find itself a way out of the insect-vector body into a new healthy tree, spreading the PWD; this is the called Primary Transmission (see Figure 1.3) [4].
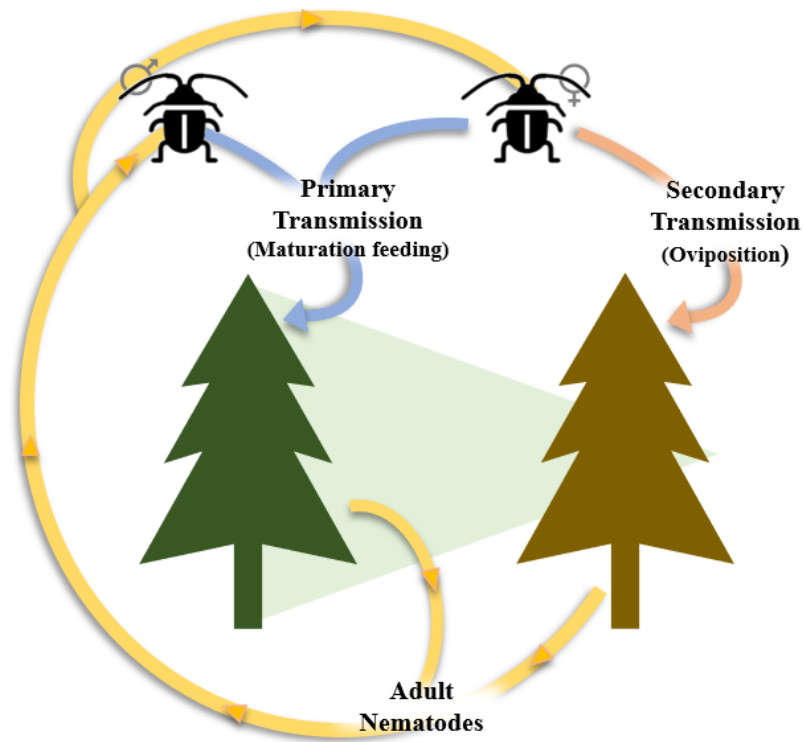
*Figure 1.3: Insect-vector transmissions of the PWN, modified from reference 4.*

To be able to oviposit, as explained earlier, females need dying or weakened pine trees, either by abiotic agents (for example, forest fires) or by biotic agents (such as other insects with which they share the host flora species), this is when a Secondary Transmission may occur (Figure 1.3) [4]. From these interactions with the PWN, and by transmitting it, the insect had acquired the ability to indirectly kill the pine trees he needs to continue to reproduce [9].

Concerning the breathing apparatus of the insect, even though it is the main access of the nematode to its vector, there are sparse information of its anatomy. The existent descriptions are general and refer a great variability among larvae vs adults and between genera [17], so the main characteristics will be further presented in the next subchapter (1.2.1) once they are transverse to the other species that will be subject of study.

### 1.3.1 Other Pine tree colonizers and the breathing apparatus

The beetles in the *Monochamus* genus are the most important vectors of the PWN and, until now, the only ones confirmed in field and laboratory observations [4], but they are not the only ones colonizing pine trees. Other genera of the Cerambycidae and other Coleoptera have been found to carry *B. xylophilus* in, or on, their bodies, namely *Acalolepta, Acanthocinus, Amniscus, Arhopalus, Asemum, Corymbia, Neacanthocinus, Rhagium, Spondylis, Uraecha, Xylotrechus* and *Chrysobothris, Hylobius* and *Pissodes*, but there is no evidence that any of those have a role as vectors in the dissemination of the nematode [1].

During the monitoring surveys for *M. galloprovincialis* in PWD infestation sites in Portugal, an enormous number of other insects were collected from traps, as, *Arhopalus syriacus* (Reitter, 1895), *Acanthocinus griseus* (Fabricius, 1793), and *Pogonocherus perroudi* Mulsant, 1839, etc. which are among the species with the highest number of collected individuals [i]. Even though there is no evidence that any of these species works as a vector, once that the interaction between insect vector and the PWN is not fully understood, we can recognized the importance of studying also other species once that pine trees are not colonized just by *Monochamus* beetles, but also by a variety of others relatives that share, not just the host and geographic distribution, but also some life cycle and anatomic features, such as the species named before (consult Appendix I and Annex II for more information). Since the introduction of PWN in Portugal, also those species, have been living alongside with the nematode and have been indirectly harmed by the decay of host trees, even if in a lesser extent. Comparing its anatomy can provide valuable data that may bring some light to these complex interactions.

Regarding the breathing apparatus of these insects, and alike what happens with the vector species, there are sparse information of its anatomy. The respiratory system of insects is composed of air-tubes, known as tracheae, that ramify, through the organs and appendages, into finer branches termed tracheoles [18], that can reach about 0.2-0.3 micrometres (µm) in diameter, transporting the oxygen that enters through the spiracles [19], the paired, lateral body openings.

The General Textbook of Entomology [20] refer that in Coleoptera, are present up to ten pairs of spiracles, two thoracic and eight abdominal; the first pair can be found between the prothorax and mesothorax and the remain pairs are metathoracic and abdominal in position. In some Coleoptera, the eight pair of abdominal spiracles, is either absent or vestigial, and non-functional [20].

Generally, the mature tracheal system has a definite fundamental pattern. The lateral longitudinal trunks present as a pair, in general, connects all the spiracular trachea from the first thoracic spiracle to the last abdominal spiracle and are usually the largest trachea in insects. Their lengthwise size and immediate connection with the spiracles make them the major avenues of air circulation. The tracheation of the insects' head, proceeding from the first thoracic spiracle, is different from that of the other spiracles once that from these are originated the tracheal supply, not only of the prothorax and mesothorax, but also of the head and all its organs. Usually it is composed of two principal pairs of head trunks, one of these on each side as a dorsal and a ventral head trunk [17]. These are the main features of the breathing apparatus that are expected to be observed in the specimens to be studied.

---

[i] for more information concerning the data from the monitoring surveys in Portuguese infestation sites, see Annex I

## 1.4 Methods approach

Understanding the morphology of anatomical structures is a cornerstone of biology [21], and therefore ecology and its variants, as it provides the necessary knowledge to understand functional features and its role in the co-evolution and interaction between species. To isolate the structural features of the vector that may be determinant for the role he plays in the spread of the nematode across host trees, becomes essential to be able to observe those features and to compare them among vector and non-vector species.

Classical methods such as histological serial sections combined with fluorescence or confocal laser scanning microscopy [22] and dissections were the only available anatomical techniques and drawing were used for illustrating the morphological findings [23], now replaced by photographs. Such techniques have provided a wealth of data, but are prone to artefacts and distortion of tissues and can be problematic due to destruction of the sample and are costly in terms of time and effort [23,24]. More importantly, physical slicing can cause deformation of internal anatomy with loss of information especially affecting the spatial relation of the studied structures in their natural anatomical context [22], a critical limitation when precise spatial data are required [21] like in this case where it is intended to study tiny hollow vessels such as tracheas.

Until the late decades of 20th century, microscopy was the only method for examining external structures; Scanning Electron Microscopy (SEM) and microphotography are an excellent tool for the documentation of surface structures and frequently used by entomologists; the strongly increased depth of focus was a strong argument in favour of SEM compared to light microscopy [23]. In the new millennium, insect morphology and systematics regained momentum with new technologies becoming available, especially, micro-computed tomography (Micro-CT) and computer-based 3D reconstruction. Modern techniques like confocal microscopy, magnetic resonance imaging (MRI) and Micro-CT provides effective non-invasive methods that can overcome the limitations of classical methods and have been shown to be valuable tools for the visualization of internal anatomical and structural complexity, being used, for about 10 years now, to study arthropod anatomy as it allows high resolution analyses of small areas of interest [22,25]. But each of these has its limitations, including sample size, resolution limits, and difficulty visualizing soft tissue [21].

Despite the limitations, these tools had become important and the demand for this kind of investigation is increasing with the necessity to study the spatial arrangement of various organ systems such as musculature [26], respiratory system [27], alimentary system, circulatory system and even nervous system [28]. Such cases where became possible to define spatial relationships and variation in size, shape and proportions of individual structures [24], with satisfactory results.

In this particular case, we have two main goals; 1) to characterize spiracles (measures, existence, or not, of bristles) by Scanning Electron Microscopy (SEM) and 2) to observe the tracheal system in order to characterize it (its length, ramifications, etc.) using Micro-CT and 3D reconstruction software. To fulfil these goals proposed it is necessary to gain experience in the techniques to be used and at the same time, it is most important to adjust those same techniques to the type of samples that are going to be studied. With that in view, the first task was to understand the techniques and then to prepare our specimens for those same techniques.

### 1.4.1 X-ray Micro Tomography

Micro-computed tomography (Micro-CT) is a recent powerful tool for the study of biological material. This technique produces high resolution (micron or sub-micron) images that can be used to generate three-dimensional (3D) models of samples, as smalls as a pinhead. It is based on the same principles of a computed tomography used by CT scanners in hospital examination [25].

The main difference is that, in Micro-CT, the sample is placed in the path of a finely focused X-ray beams (electromagnetic radiation with wavelengths of 0,01 and 1 nanometre) that passes through the sample, to a X-ray-to-light converting scintillator, through the detector (a light imaging device, usually a charge-coupled device - CCD - similar to the one of a digital camera), then to a controlling computer (as schematized in Figure 1.4) [29], and a two-dimension projection (radiography like) of the sample is obtained [22]. To produce a virtual volume it is necessary a series of projections (or scans) of the sample; while the sample rotates, images of multiple angles are shoot in a sequence, by at least 180º [22,25] – Acquisition step. To reconstruct sample details in 3D, an inversion algorithm is used (NRECON®) – Reconstruction step – and hundreds or thousands of slices of the object are obtained. After that, by combining the obtained slices in a visualization program (CTVOX®) with a specific geometrical function, integrated in the Micro-CT systems, it can be created a virtual volume of the sample [25].
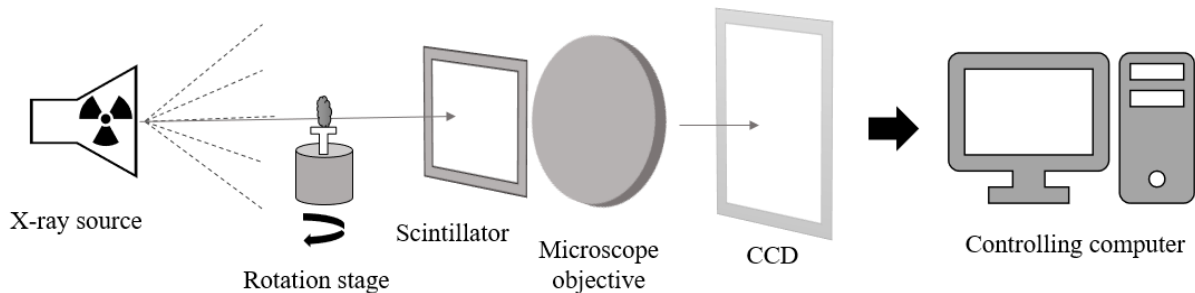


*Figure 1.4: Schematization of a Micro-CT scann; the sample is placed on the rotation stage in the path of the beam, then the transmited x-ray energy is converted to visible light by the scintilator and projected onto the CCD by a microscope objective; modified from reference 29.*

It enables microanatomical investigations because of the way that X-ray interacts with different materials (or molecules)[24]. According to Lambert Beer law, the absorption of x-rays depends on the nature of the materials (chemical composition), their thickness (absolute size of the tissues) and their compactness (existence of empty spaces or the distribution of constituents). The intensity at which X-rays pass through the sample is affected by its composition; the X-ray absorption increases with atomic number of the elements of a sample (such as its density), resulting in relative variance in the electromagnetic waves, that way very distinctive material can be easily distinguish [24,25]. The problem relays in differentiate structures with similar elemental composition (and for example, highly hydrated tissues); contrast between materials can be improved by using the right fixation and dehydration processes, and even by applying a contrast agent such as a staining agent [29] or a metal (like osmium, gold, gold-palladium) it becomes possible to isolate even tiny structures like the air-filled tracheas of an insect from the surrounding muscle fibres [21,23–25].

After the acquisition and reconstruction steps there are various tools to be used in various posterior analyses. The three-dimensional specialized software that allows viewing virtual sections of the sample that is a two-dimensional image that can be moved and rotated through the scanned volume to explore details. Volume rendering enables the visualization of the contents of a volume, based on the colours and transparency assigned to voxels (it is the equivalent to a 3D pixel) depending on their intensities value. It can be used to display some features while removing others if their densities differ, also can provide quality descriptions and linear and two-dimensional measures [25]. Features can also be

individualized and labelled (also called Segmentation): by using the automatic thresholding it is possible to label regions if there is high contrast between adjacent sample regions, for example bone next to a muscle, while lower contrast borders require increased user interactions to obtain reliable segmentation results [25].

Some papers refer that, despite the fact that tomography is non-invasive, the insect samples can present some internal deformation due to movement of the specimen or the heating caused by the beam in the Micro-CT sample chamber [21]. We discovered in the literature, for example in papers of Alba-Tercedor and his team [30,31], that has a lot of experience with Micro-CT scanning, that before the scanning, in order to avoid, or at least minimize, those inconvenient, some investigators stabilize the samples priori to imaging, for example by critical point drying, greatly reducing the chance of internal tissues and organs to collapse and thus maximizing the scanning success.

Even more, structures such as tracheal tubes are more likely to deform and, in some cases, appear to have disappeared entirely. Insect's tracheal system consists mainly of a single layer of cells that range in size from hundreds to less than a single micrometre in diameter and due to their function as distributers of gases directly to the tissues, tracheal tubes form a dense network that runs throughout the entire insect body. The absence of trachea in the tomography scans can be an indicator that some aspect of the fixation went wrong, rendering the tubes unviewable [21].

That is the major obstacle that we must overcome, to find a method that would secure these structures. Within the consulted literature, it is referred that dehydration by the standard procedure of introducing the sample for two hours in each of a series of ethanol solutions with increasing percentage of concentrations (80%, 90% and 100%), dried before the scan procedure by a standard critical point or by submerging for 24 hours in hexamethyldisilane and air drying overnight, produce very satisfactory similar results [31,32]. Others choose to perform the dehydration in a graded series of acetone and the fixation agent too varies from author to author such as the killing methods when working with living animals.

Another challenge is to centre accurately the sample; the specimens must remain perfectly still while images are collected once that a small variation of the central position can cause the projection image to come out of focus due to the rotation during the scan procedure that magnifies that small variation [30]. To overcome these inconvenient, small samples can be fixed to the sample holder with plasticine and others are even glued to avoid any movement [21,30].

Our samples, specifically *M. galloprovincialis* specimens, were consider as large ones, for both Micro-CT 's and SEM's sample holders, and even for the application of fixation protocols. Because of that, extra precautions and previous preparations were needed, such that will be further explained in chapter 2 Methodology.

### 1.4.2 Scanning Electronic Microscopy

Scanning Electronic Microscopy (SEM) is used for the observation of surface structures, and has a strongly increased depth of focus [23] allowing the user to photograph the interest areas with great detail and save the data for posterior analyses. It is based on raster scanning of the object surface with a focused electron beam that flows in a chamber under vacuum (e.g. $10^{-5}$ Pascal). The electrons emitted by the filament, named primary electrons, does not pass through the specimen, instead quickly scan the surface of the sample and by interacting with the sample's molecules promote the emission of electrons. Those, called secondary electrons [33], emitted by the molecules excited by the electron beam, are accelerated towards a scintillator located laterally to the sample. The scintillations produced by the impact of secondary electrons on the scintillator (or detector, see Figure 1.5) are then conduced to an amplifier. The electric impulses generated there are led to a screen where a black and white image is displayed. [34]
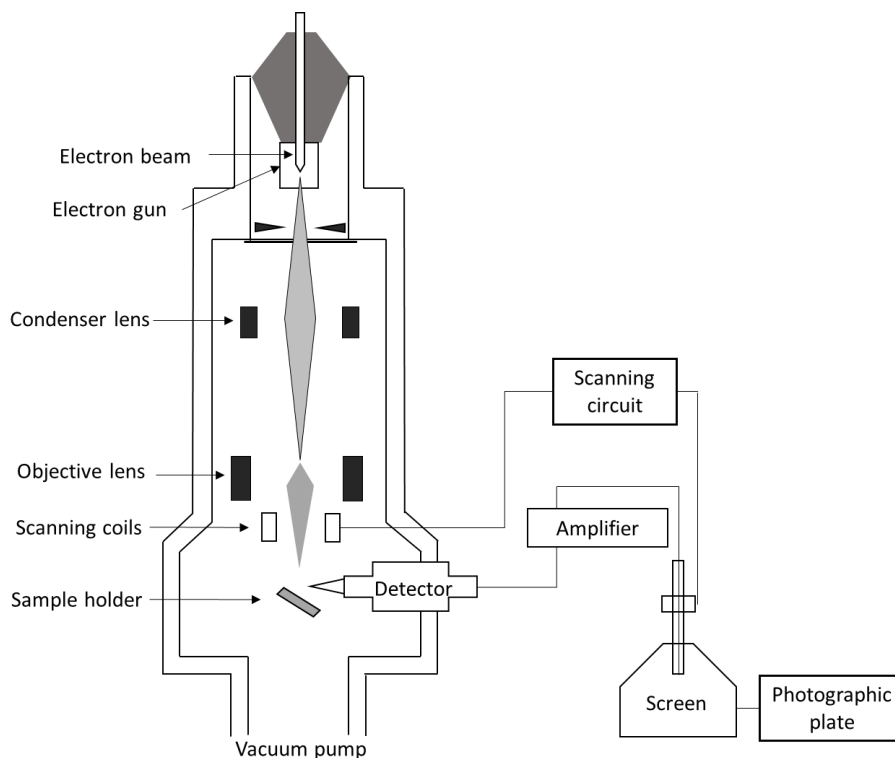


*Figure 1.5: Schematization of a Scanning Electronic Microscope; electron beam is focused by the condenser lens until it reaches the sample holder promoting the emission of electrons of the samples molecules; based on schemes from refence 33.*

The obtained images of the surface can reach resolutions below 1nanometer, a strong argument in favour of SEM compared to light microscopy [23]. Another useful tool is a rotatable sample holder that makes possible to obtain all standard views with a single specimen in a single data collection and in a homogenous background.

As in Transmission Electronic Microscopy (TEM), in order to endure the scanning process, the biological material must be chemical fixated to stabilize the cell's structures, and dehydrated to remove water from the tissues softly than would happen if the sample was placed in the chamber under vacuum without any treatment, which would cause structures to collapse. Those treatment procedures can be one of many possible and suitable ones (see Figure 1.6) [33]; the choice normally depends on the material availability of the laboratory but also is important to have a clear idea of the different procedures.
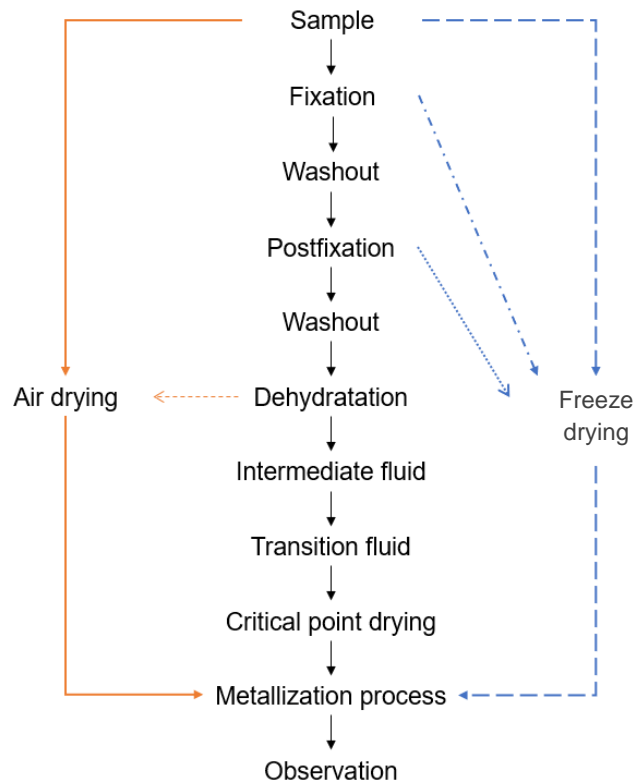
*Figure 1.6: Different treatment procedures suitable for the preparation of biological material for SEM or TEM observation, the different arrows and colours represent different treatment paths; based on a scheme from reference 33.*

In chemical fixation (or fixation), for example, the best fixative for a tissue is the one that enable to preserve the most cell structures possible, avoiding decomposition by stopping any biochemical process. The goal is to conserve the sample in its natural state for the purpose of observation reason why one of the biggest problems in the preparation of biological material is to choose a suitable one. Moreover, pH, temperature, tonicity of the fixative solution and the duration of the fixation are important aspects to consider [33] and to be discussed further in chapter 1.3.2.1. Fixation and Critical Point Drying.

One more step before SEM is crucial, the Metallization process. Once that the basic composition of biological material does not favour the emission of secondary electrons, to achieve a good quality observation of the sample, it is necessary to cover the specimen with a dense and electric conductive metal, usually being used gold or palladium-gold [34]. In a Metallization device, the sample is placed in a holder inside the chamber, a gold plate is attached to the cathode while the sample holder is placed on the anode. When the chamber is closed, an electric current is formed, and charged particles of the metal attached to the sample covering its surface, being the sample ready for SEM.

### 1.4.2.1 Fixation and Critical Point Drying

Chemical fixators can be one of two kinds, coagulant and non-coagulant. Among the first type, there are alcohol, acetone and acetic acid, and among the second one there are the aldehydes, such as formaldehyde and glutaraldehyde, and osmium tetroxide. It is normal to practice a double fixation with an aldehyde, a pre-fixation usually with glutaraldehyde, followed by a post fixation with osmium in to stabilize the primary components of cell structures [33]. The stability of the fixated molecules depends on the concentration of the fixation agent, buffer solution composition, process' duration, temperature and sample's dimension. Also, the fixation should occur in a neutral buffer solution (pH 7.2 – 7.5) at a temperature of about 4º Celsius to avoid post-mortem alterations. Even more, the duration of fixation must be adjusted to each type of sample and result from a compromise between a good fixation outcome, its duration and the resources used, and for a good fixation outcome, the fresher the biological material, the better [33].

Critical Point Drying (CPD) is an established method of drying used for strengthening of biological structures and tissues before a Scanning Electron Microscope examination [35] and have been used for Micro-CT samples as well [26]. The critical point of a substance is obtained at specific conditions of pressure and temperature. A part of the process includes the occurrence known as the continuity of state for which there is no apparent difference between the liquid and gas state of a medium and the surface tension between this interface is reduce to zero. At this point, the medium exhibits specific properties and has an intermediate behaviour between that of a liquid and a gas, particularly, has densities like a liquid while the viscosity and diffusivity are closer to that of a gas. This condition of zero surface tension can be used to dry biological specimens, avoiding the damaging effects of surface tension.

Between the most used substances for CPD there is Hydrogen, Carbon Dioxide, Nitrogen, etc. (see Table 1.1 [36]). In biological specimens, as the ones in study, the main concern is the removal of water from the tissues; if not done previously to the SEM examination, it would cause the structures to collapse due to the vacuum created in the SEM specimen chamber [35]. As the critical point for water (+374°C and 221.5 bar) is inconvenient since it would cause heat damage to the specimens, something that is not desirable too, once the intention is to maintain structures the most stable possible, it will be used Carbon Dioxide for CPD.

*Table 1.1: Critical constants for most used substances in critical point drying, adapted from reference 36.*

| Substance | Temperature (◦C) | Pressure | |
| --- | --- | --- | --- |
| | | P.S.I | Bar |
| Hydrogen | -234.5 | 294 | 20.3 |
| Oxygen | -118 | 735 | 50.7 |
| Nitrogen | -146 | 485 | 33.4 |
| Carbon Dioxide | +31.1 | 1072 | 73.9 |
| Carbon Monoxide | +141.1 | 528 | 36.4 |
| Water | +374 | 3212 | 221.5 |

Carbon dioxide ($CO_2$) is the most widely used as a supercritical fluid because it is cheap, chemically inert, non-toxic and non-flammable, readily available at high purities and at low costs, it has low toxicity and $CO_2$ critical point is easily accessible at a critical temperature of 31,1° C and a critical pressure of 73,9 bar [35] (see Table 1.1 ).

However, $CO_2$ it is not miscible with water (present in all biological material and in alcohol solutions that are used for conservation), and therefore, a third medium must be involved, commonly Acetone, which is termed the intermediate fluid. Therefore, before the drying process and after the fixation, the samples must be dehydrated, which means, to have water removed from the tissues. This dehydrated state is usually achieved by submerging the material in a graded alcohol or acetone series solution of 10% V/V to a 100% V/V concentration [33,35].

After that, it is possible to convert our transitional fluid, $CO_2$, from liquid to gas without surface tension at critical point and without damaging the specimens becoming ready and steady for both SEM and Micro-CT procedures.


### 1.4.2.2  Lyophilization

Lyophilization, freeze drying or cryodessication, is other process suitable for strengthening and stabilization of biological material to a level that it will no longer support biological growth or any chemical reactions [37]. The process consists of three stages: Freezing, Primary Drying and Secondary Drying. The freezing must be rapid to avoid the ice crystals formation inside the cells. Then the sample is heated (by conduction or radiation or both) under vacuum so that the frozen liquids sublimes and only the solid components remains – Primary Drying. The application of vacuum allows the free migration of water vapour from the frozen mass, which may be regarded as a diffusion process, reason why it is a relatively slow process. The slow sublimation of the ice avoids damaging the tissues, however, occur a reduction of about 15% of the volume of the tissues [33]. Secondary Drying allows the water that did not get frozen to be removed by a desorption process, which means that a substance is released from or through a surface [38,39]. The objective is to reduce the water content (moisture) to a level considered optimal for stability, less than 1% [37].

The lyophilization chamber is made of stainless steel, highly polished and well insulated and provides the temperature and pressure suitable to conduct each step of the process. A control system is needed to set up the temperature and chamber pressure, depending on the product and the whole process can vary from hours to days to be completed [37].

## 2 Methodology

Considering the specifications of the different techniques to be tried, and due to the fact that we wanted to observe both structures (trachea and spiracle) in each specimen in both states of development (pupae and adult), it became imperative to applied the techniques in an order that would not cause the insect destruction. Reason why we initially thought of doing Fixation and Critical Point Drying, followed by the Micro-CT scanning, then isolate the specimen abdomen so it could be covered in gold and fit in the sample holder to be properly photographed in SEM. We stablished that it would be analysed ten pupae and ten adults of each species.

All insects were obtained from naturally infested *P. pinaster* trees, collected at Península de Tróia (Grândola) and Companhia das Lezírias (Samora Correia). Portions of trunks and branches of felled trees were surveyed, and the parts with cerambycid colonization were cut in one-meter long sections and transported to the laboratories of the Instituto Nacional de Investigação Agrária e Veterinária (INIAV, Oeiras, Portugal). The logs were cut into smaller sections and the pupal chambers opened manually, using a hammer, knife and axe, to collect the last instar larvae from the pupal chambers, where they overwinter, and identified if belonged to the different target species and individually placed on filter paper disks inside disposable 55 millimeter diameter Petri dishes, to facilitate the moulting to pupae and later, to adults.

The first insects had been captured from host trees in the previous season and were preserved in ethanol (70%) for few months before we started to work with them and that is why they were used in SEM and Micro-CT preliminary tests. In both SEM, Micro-CT and Fixation and Critical Point, more than one procedure was tried, with some alterations, to adjust the protocol and choose the one that could guarantee the best outcome considering a time vs resources compromise.

All the insects were named with an identification code (ID) composed by the initial letters of the specific name (Mg for *M. galloprovincialis*, Ag for *A. griseus*, As for *A. syriacus* and Pp for *P. perroudi*), followed by a capital P if a pupae, and its personal number. For preliminary tests specimens, the numeration starts in 000, for the specimens fixated and critical point dried is 0000 and for the ones submitted to lyophilization the numeration starts in 0030.

### 2.1 SEM

*M. galloprovincialis, A. griseus* and *A. syriacus* insects, due to its length, do not fit entirely in the thumbtack usually used to place the samples in the microscope sample holder, reason why we decided to isolate the insect abdomen and that this would be the last method to be performed.

The Preliminary tests were conducted on two groups of insects; the first group of specimens (*M. galloprovincialis*) were put out of the flasks and dried overnight in the lab at room temperature; by removing the elytra, wings, legs, head and thorax, the abdomen was isolated; with a double side carbon tape, it was fixed in a metallic thumbtack, followed by metallization with gold and then SEM scanned.

For the second group of specimens (*M. galloprovincialis* and *A. griseus*) the alcohol in the flasks has changed for new alcohol 70% and leave it overnight, this was repeated if the alcohol gained a yellow colour until it became clear; the specimens were Critical Point dried and by removing the elytrum, wings, legs, head and thorax, the abdomen was isolated; with a double side carbon tape it was fixed in a metallic thumbtack, followed by metallization with gold and then SEM scanned.

All the specimens were scanned in a Jeol JSM 5200LV Scanning Electronic Microscope and were placed in the metal thumbtack in the same way, dorsal view up so the spiracle would be visible, and were photographed from top-bottom left to bottom-top right, and the spiracles were numbered as shown in Figure 2.1.A, so they could be properly identified. Later one, the photographed specimens where the ones fixated and critical point dried or lyophilized, according to the protocol described in chapter 2.1.1 and 2.1.2, and all imaged spiracles were analysed as next described.

To analyse the images of the photographed spiracle and get it measured it was used the software ImageJ (version 1.52i, see Figure 2.1.B for reference). The first step was to calibrate Image J by setting the scale (menu "Analyze" > Set Scale) from pixels to micrometres using the scale bar from the instrument [40]; to avoid errors, and once that there was images with different scales, this calibration process was performed for each image [41]. Using a Pen Tablet and the Polygon selection mode (Figure 2.2) it was possible to accurately mark the spiracle margins; sometimes this margins are not so clear to distinguish, so by applying the process "Find Edges" (Process menu > Find Edges) it is possible to illuminate the boundaries of the structures which in some cases simplifies the analyses. The ROI Manager (ROI as region of interest, the one that is marked by the user) saves the marked region, in this case it is the spiracles margins, so it can be adjusted if needed, and with the Measure Tools it is possible to obtain the Perimeter (length of the outside boundary of the selection) and Area of the section (by default, area is calculated in square pixels, with spatial calibration it is obtained in the calibrated units such as square millimeter, for example),  as well as its major length, minor length, and other features, displayed on the results screen.

By selecting the option "Shape descriptors" in the Set Measurements menu, it can be obtained some features regarding the shape of the selection, such as Circularity (calculated as $4\pi*$area/perimeter$^2$); a circularity value of 1.0 indicates a perfect circle, as the value approaches to 0.0, it indicates an increasingly elongated shape [42]. Beside the measure of the spiracle total area, it was also measured the area of the spiracle not covered by bristles (the called open area) with the freehand selection tool.  The measures of the spiracles were exported to an Excel file and saved for posterior statistical analysis.
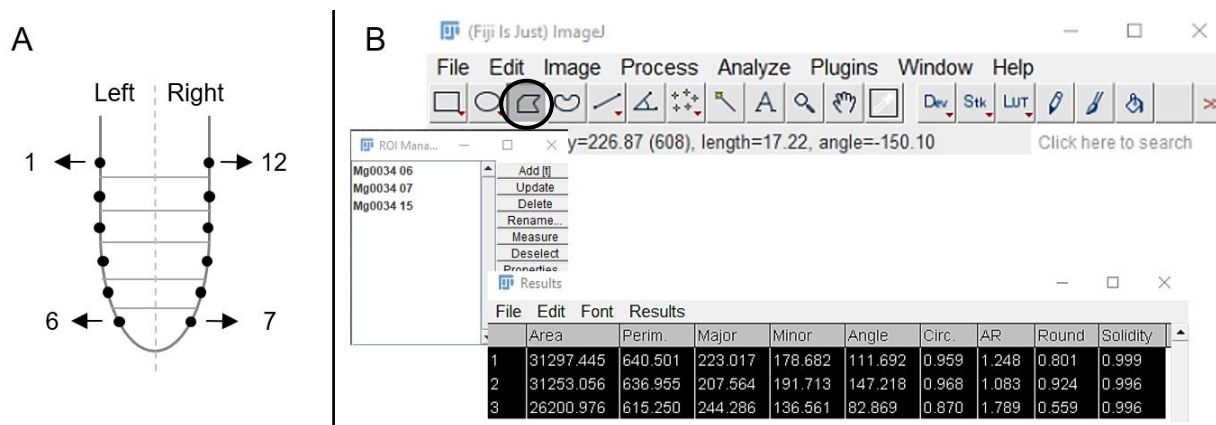


*Figure 2.1: A - schematization of the numeration of the spiracles (not at scale); B – ImageJ (2.0.0-rc 68/1.52i) menus and Polygon section tool (highlighted with a circle) used to mark the spiracles.*

### 2.1.1 Fixation and Critical Point Drying

The insects to be sacrificed were collected as larvae from pine tree logs cut at PWD control sites and maintained in laboratory. The hatched larvae were put in individual Petri dishes with filter paper and kept in the dark inside cardboard boxes at room temperature, as done by Naves et al. 2008 in their work [7], where were kept until became pupae and adults .

The fixation protocol used in this work is adapted from the ones used in the work of Figueredo *et al.* 1994 [43]. For the first fixation event, the living material was submerged in an 1,5% Glutaraldehyde (GA) in 0,05M sodium cacodylate buffer solution (pH 7,4 - 7,8) for about 45 minutes at room temperature in a platform shaker (Innova 2300). After 10 minutes under vacuum (26mm Hg) the fixative was substituted by 3% GA in 0,1M sodium cacodylate buffer solution, for six hours in the stirrer at room temperature.

Glutaraldehyde, the first fixative agent used, bonds with lipids and proteins of the cell's membrane stopping the cells development in the moment at which the fixation occur. Sodium cacodylate buffer solution maintain the pH at a neutral point and the osmolarity (or osmotic concentration) to enable a proper diffusion of the fixative agent into the samples' cells preventing cell plasmolysis. The second fixative to be used is osmium tetroxide; it will bond with other major cell component, peptides. Osmium tetroxide is prepared in a pure water solution once it easily forms black compounds if contact with other substances which would make it unavailable to bond with the cells' molecules of interest[33,43].

Washout is necessary to remove any remains of the fixative that did not react with the samples tissue. It should be breve enough and done with the same solvents used for the fixation solutions (glutaraldehyde – sodium cacodylate, osmium tetroxide – pure water) to avoid any unwanted extraction of non-fixed material due to drastic alterations or a consequent decrease of the sample volume [33].

The material was then divided in two groups of four specimens each. The first group (one larva, 1 pupa, 2 adults of *M. galloprovincialis*) was rinsed (washout) in the same buffer solution, 3 times with 5 minutes apart and post-fixated with 2% osmium tetroxide aqueous solution and went for one more hour in a stirrer. The second group (1 larva and 3 adults of *M. galloprovincialis*) stayed in the stirrer during this process. After that, the samples were moved to the fridge where they remained for five days.

The 2nd group, was then rinsed in the same buffer (3 times with 5 minutes between each one) and post-fixated with 2% osmium tetroxide aqueous solution where it remained during the day in the platform shaker until it was finally moved to the fridge. After 24 hours, both 1st and 2nd group were washed three times with pure water with 10 minutes between each wash and then were dehydrated in a graded acetone series (10% V/V acetone to 100% V/V acetone) with 20 minutes apart each bath. After 20 minutes stirring in 100% acetone, it was replaced for 100% acetone for a second time. Before critical point drying, and after the dehydration process, the samples can remain in the fridge for several days without compromising the material.

The 1st group was delivered to the technician for critical point drying and then returned for observation. During that time, the 2nd group remained in the fridge being later delivered to the same technician for critical point drying. Before that, antenna, legs, elytra and wings were removed from the adult specimens while they remained submerged in acetone.

A second fixation event occurred with a few modifications; four pupae and five adults *M. galloprovincialis* were submerged in 1,5% GA in 0,05M sodium cacodylate buffer solution (pH 7,4-7,8) for about two hours at room temperature in the platform shaker; after 10 minutes under vacuum (36mm Hg), the fixative was replaced by a 3% GA in 0,1M sodium cacodylate buffer solution and were placed in the fridge for 24 hours. The specimens were rinsed with the same buffer solution (three times, 10 minutes apart) and post fixed with 2% osmium tetroxide solution where remained for five days.

Then, they were washed with pure water (three times, 10 minutes apart); with the specimens still in pure water, antenna, legs, elytra and wings were removed from the adults. Afterwards, the samples were dehydrated as described before, in a graded acetone series (10% V/V acetone to 100% V/V acetone) and left in the fridge in a second 100% acetone solution until critical point dried.

The next fixation events with *M. galloprovincialis* and *A. syriacus* specimens (pupae and adults) were performed like the last described but post fixed with 0,5% osmium tetroxide solution, maintaining all other steps of the procedure; for *M. galloprovincialis,* were chosen the smallest ones to be sacrificed from this point forward, in an attempt to improve the fixation outcome by reducing the volume in which the fixative agent had to impregnate.

For *P. perroudi* specimens, once they are the smallest ones, a few adjustments were made in the protocol, concerning essentially the duration of some steps: both pupae and adults were submerged in 1,5% GA in 0,05M sodium cacodylate buffer solution for only one hour and stirred at room temperature in a platform shaker and then placed during 5 minutes under vacuum (26mm Hg) and remain only for three days in 0,5% osmium tetroxide solution; all the other steps were the same.

All the specimens, after fixated, dehydrated and critical point dried (CPD), were observed in an optic microscope; the ones that seemed well fixed were then sent to Micro-CT in individual Eppendorf tubes or to SEM, with their individual codes attached; the ones that collapsed during the Critical Point drying were stored individually in Eppendorf tubes as well.

### 2.1.2  Lyophilization

Being this a less time consumer process for stabilization of living material, in order to assess its suitability for our samples, we separated some pupa and adults' specimens of *M. galloprovincialis*, *A. syriacus* and *A. griseus* that were frozen in their Petri dishes in a freezer at a temperature of -18°Celsius. After 2 or 3 days freezing, the samples were moved to a lyophilization chamber where the primary and secondary dryings occurred until the water content of the sample was nearly 1%, which last for about 3 days.

The specimens were also observed in an optical microscope to remove the appendages, as done with the fixated ones. The specimens were divided between SEM and Micro-CT and sent to the technicians with their individual codes and the ones that collapsed were stored in Eppendorf tubes.

## 2.2 Micro-CT and Segmentation

To visualize the tracheas, we tried different conservation processes. Initially, were scanned a few specimens that had been rehydrated, others only air dried after dead or freeze dried. The insects, from the first and second group fixated as described in the previous sub-chapter, were scanned along with some others critical point dried after being washout in ethanol or acetone.

For scanning the specimens were mounted in a plastic container, an Eppendorf tube, which has a low density that makes it transparent to X-rays [44]. It is placed as tight and straight as possible for the specimen does not move during the Micro-CT scan and fit properly in the camera range, then it is put in the sample holder inside the CT scan (SKYSCAN 1174 from BRUKER®). The sample chamber is closed, and a previous radiography of the specimen is obtained in the CT software on the controlling computer, and from there the parameters for the Micro-CT scan are adjust (consult Appendix II), such as the Rotation Step (the degree at which the sample will rotate and will be shot), the frame averaging and image pixel size. After the Acquisition step and the Reconstruction step (already described in chapter 1.3.1), a first virtual volume of the sample is ready to be worked and improved.

Once that the acquisition was made inside an Eppendorf tube, a primary segmentation is required to digitally remove the material [45]. BRUKER® software CTAnalyzer (CTAn) is the one used in the cleaning process. Loading the dataset into CTAn it can be visualized the virtual volume as slices viewed from a transversal section of the insect body. The loaded images are presented in a gray scale based on the intensity of the voxels, but for a better visualization of the details, a colourful filter can be applied. Using the Region of Interest (ROI) editing function it is possible to select a region of a specific slice, in the shape of a geometric form (circle, square or ellipse) or a freehand draw, where a certain detail is of interest to be individualized. The software also allows the marked ROI to be interpolated between marked slices, so the user does not need to define the ROI shape in all the slices of the entire virtual volume [46]. After setting the upper and lower limits of our ROI, a new dataset can be created as a new Volume of Interest (VOI) containing only the marked ROI, this is the called Segmentation. This procedure was reproduced, primarily, to remove the Eppendorf halls to isolate the insect body of the specimens we worked on, and afterwards to try to isolate the tracheal trunks as shown in Figure 2.2, where the trachea ramification is highlighted by a red circle corresponding to the ROI.
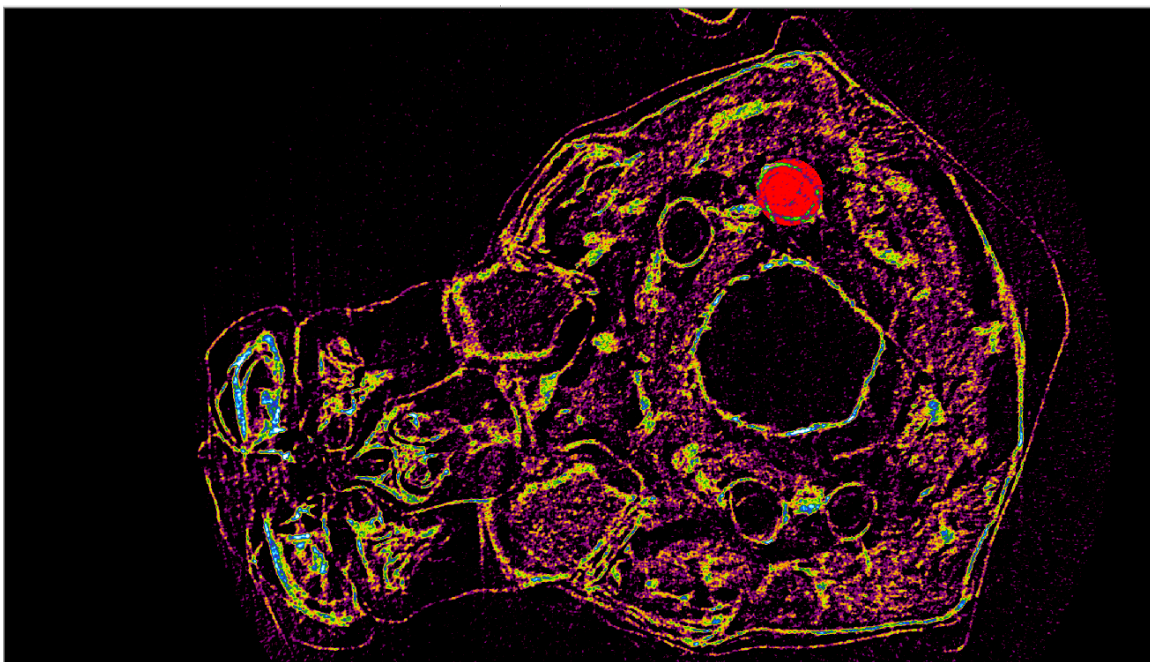


*Figure 2.2: Selection of one tracheal trunk using the CTAn ROI editing function in a 2D cross-section of the head of a M. galloprovincialis adult (Author's original).*

As already mentioned, the tracheal system is composed by at least two main ramifications alongside with the insect abdomen and four main ramifications in the head and thorax. The main limitation of the ROI editing tool is that only one ROI can be marked in each slice, which mean that by following the steps described above, it would only be possible to segment one trunk of the Tracheal system and that a segmentation and reconstruction of the entire system would take a lot of working hours to achieve because it would have to be repeated for all the main trunks and all combined afterwards.

During the search for a solution to overtake this restriction, it was found a Method Note from Bruker called "CTAn: the externally edited image format ROI" [47], a new procedure that would allow multiple ROI shapes. With this update in ROI function, a new option in ROI shape menu called "Image" is available (Figure 2.3), that allows to import a binary image (black and white image) and use it as the ROI, braking free of the one-object limitation, becoming possible to import an image with the objects of the cross section that as interest to your project. This would mean that it could be possible to mark and reconstruct the two main ramifications of the abdomen and the four main ramifications of the head with one analysis.
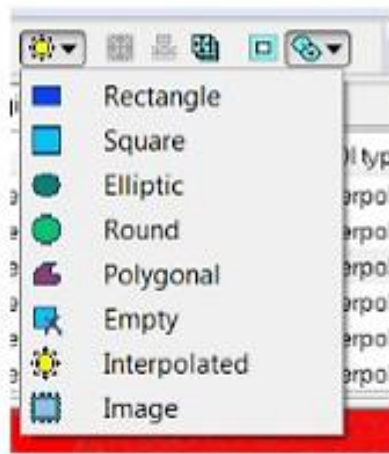


*Figure 2.3: Image format in the shape menu at the ROI page of CTAn software.*

### 2.2.1  Multiple ROI for Segmentation of the main Tracheal Trunks

After choosing one insect virtual volume dataset with detailed images, where the tracheal trunks were visible, the first step was to make a copy, in the dataset folder, the 2D cross-section image where it is needed to add two, or more, ROI shapes. This copied image is then edited, not the original one. In an image editing program (the one used was ImageJ), the copied cross-section image was load, and the outline shapes of the two (or four, depending on the section) trachea ramifications were drawn, as shown in Figure 2.4, with the Oval or Elliptical drawing tool, in the colour white, and the changes were saved.

Next step is to load the saved edited image into the CTAn and binarized, which means, make it a black and white image. Before doing it, it is important to select in the file preferences; on the "General Tab", the setting "RGB to gray" must be set as "Luminance", just then apply  "Threshold" of 254 or 255 of the gray level, which will present a preview of the binarized image with just the white drawn outline (Figure 2.5 A). Sometimes, after confirming the Threshold, a few white regions that has the same gray level, resulting from saturated pixels of the original cross-section, are shown as well (Figure 2.5 B), but those are easily removed in the following step.  In "Custom processing" repeat the Thresholding, setting it as "Global" with gray levels Low: 254 and High: 255.
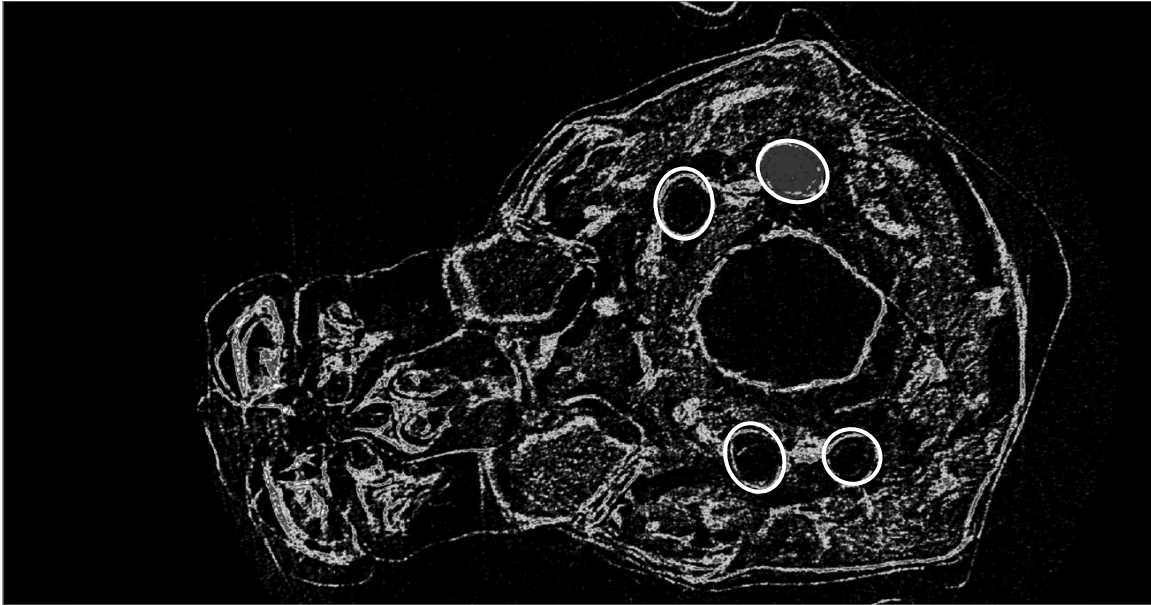
*Figure 2.4: Selection of the tracheal trunks using the oval shape drawing tool of ImageJ on a transverse 2D cross-section of a M. galloprovincialis adult (Author's original).*

To remove any white dots that still appear in the binarized image, it was been used the "Despeckle" plug in (setting the options "Type" as "Remove pores" and "2D space", "Detected" as "by image borders" and "Apply to" as "Image"). At last, after saving the ROI as a binary image, saving it as bitmaps (selecting "convert to monochrome (1-bit)" option) the binarized image correspondent to the ROI with the four (or two) trachea trunks marked (Figure 2.5 C) can be saved in a new subfolder, automatically created, called Mask.

This procedure was repeated for several cross section images to create image-type ROIs for several cross section levels as they were needed; for example, at first it were created two masks, one for the anterior cross section of the insects thorax where four ramifications of the tracheal system were visible, and other mask for a posterior cross section of the thorax where the four trunks merged in two.

To complete the segmentation, the final step was to load the original dataset to CTAn. After limiting the ROI upper and lower limits, the menu ROI shapes can be set as an "Image" type ROI on the cross-section level of one where you edited the copy image and created a Mask. Only then it can be loaded the mask previously done by clicking in "load image ROI". The volume of interest that we want to create would be a combination of ROI levels imported as binary images and standard drawn ROIs with a single shape, once that CTAn will be able to interpolate between these single and multiple ROIs. The new VOI, theoretically with all the main trunks individualized, could be normally saved.
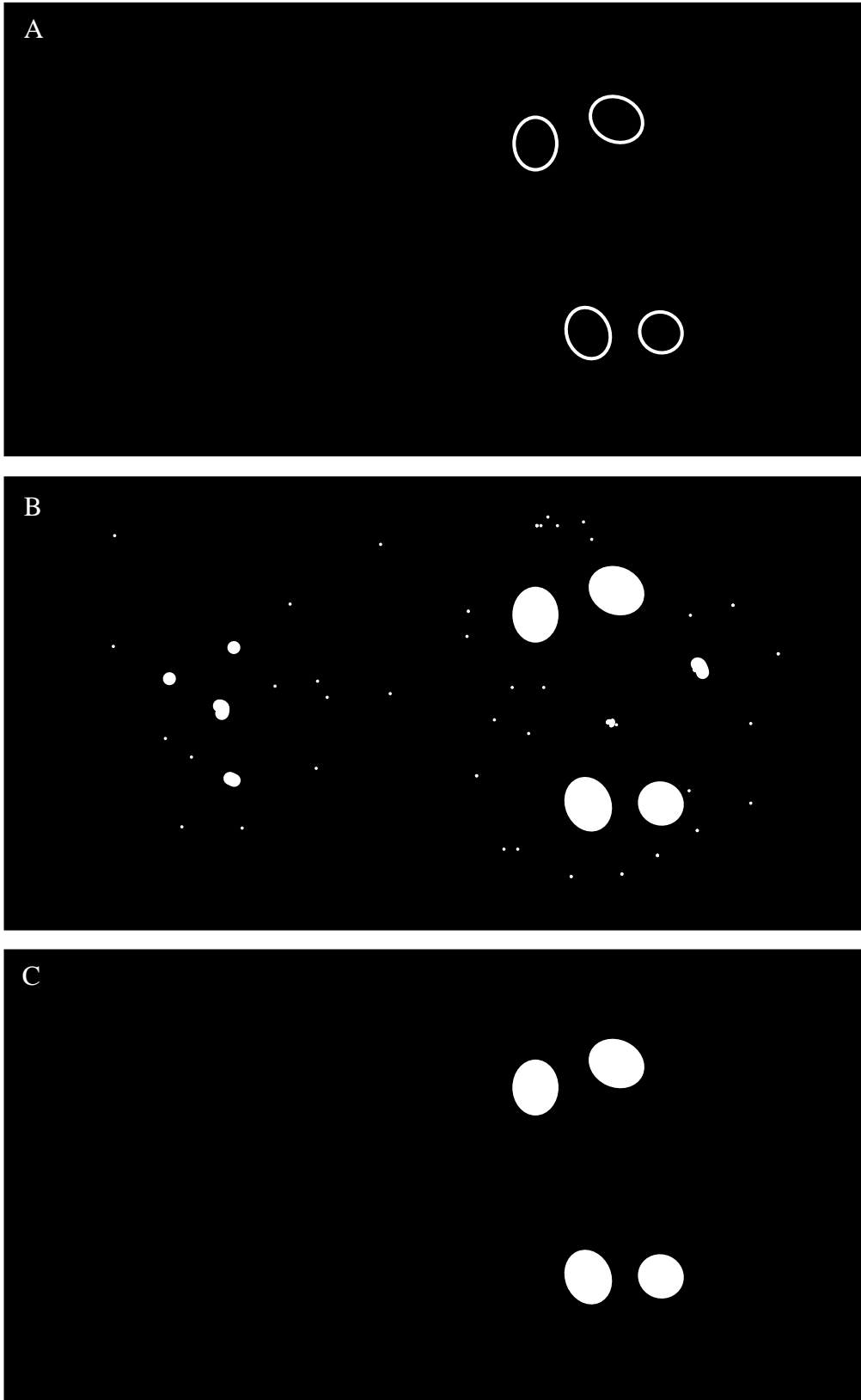
*Figure 2.5: Multiple ROI shapes drawing process, A - preview of the binarized cross-section image, B - binarized cross section image with white speckles, C – final binarized image correspondent to the ROI with the four trachael trunks marked, (Author's original).*

### 2.2.2 Tracheal Volume Estimation

In an attempt to obtain some descriptors of the tracheal system, we thought of doing an estimation of the trachea volume. To do so, we assume that the major ramifications that we could follow with the CTAn would have a cylinder like shape, and therefore the volume could be calculated as $\pi r^2 . h$ (where h is the length of the section and $\pi r^2$ the area of the circle, or area of the tracheal trunks).

While analysing the Micro-CT scans, it became clear that not all the ramifications could be distinguished alongside all the insect body, so the total length of the insect has measured as well as the length of the head, thorax and abdomen using the CTAn Measuring tool. Then, with the same tool, the area of the ramifications observed in sections of the head, thorax and abdomen, were measured as shown in Figure 2.6.

This procedure was repeated for one male, one female, one pupa of *M. galloprovincialis*, one adult *A. syriacus* and two adult *A. griseus*, one male and one female, and for several sections where the tracheas were visible; the measures were saved in Excel files for posterior calculation of the volume.
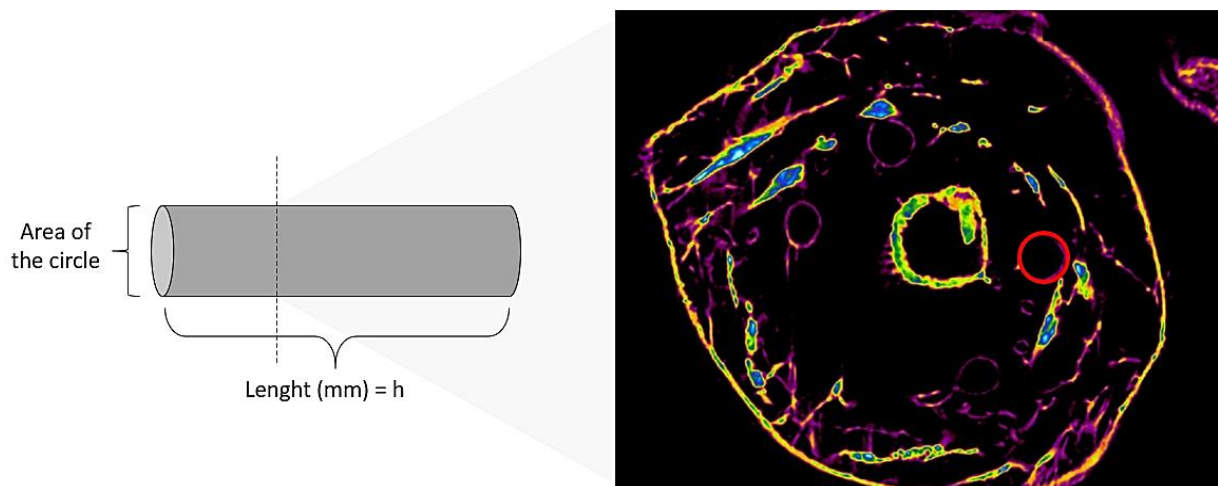


*Figure 2.6: Scheme of the measure of a trachea ramification in a section of the head of a M. galloprovincialis insect; area of the circle refers to the on marked in red (Author's original)*

# 3 Results

## 3.1 Fixation and CPD versus Lyophilization

As mentioned in chapter 2.1.1, insects had to be sacrificed for SEM and Micro-CT. Overall, were used 85 insects between the chemical fixated and the lyophilized ones, being 48 *Monochamus galloprovincialis*, 27 *Arhopalus syriacus*, 4 *Acanthocinus griseus* and 7 *Pogonocherus perroudi*. The table below (Table 3.1) shows the number of specimens prepared with each process, as well as the distribution of specimens for each purpose, observation of the spiracles by SEM or observation of the tracheal system by Micro-CT. Inside the parenthesis are expressed the numbers of specimens that collapsed during both stabilization processes and because of that were not used.

*Table 3.1: Distribution of the number of chemical fixated and lyophilized insects (M. galloprovincialis (Mg), A. syriacus (As), A. grisues (Ag) and P. perroudi (Pp)) for SEM and Micro-CT; inside the parenthesis are expressed the numbers of specimens that collapsed during both stabilization processes.*

| | **Fixated** | | **Lyophilized** | |
|---|---|---|---|---|
| **Mg** | 19 (8) adults | 9 SEM | 7 adults | 5 SEM |
| | | 2 Micro-CT | | 2 Micro-CT |
| | 20 (3) pupae | 14 SEM | 1 pupa | Micro-CT |
| | | 3 Micro-CT | | |
| **Ag** | – | – | 4 (1) adults | 2 SEM |
| | | | | 1 Micro-CT |
| **As** | 8 (3) adults | 3 SEM | 8 adults | 7 SEM |
| | | 2 Micro-CT | | 1 Micro-CT |
| | 6 (2) pupae | 3 SEM | 5 (5) pupae | – |
| | | 1 Micro-CT | | – |
| **Pp** | 3 (2) adults | | | |
| | 4 (2) pupae | | | |

From the total 60 fixated and critical point dried specimens, 20 collapsed, making unviable the observation either by SEM or Micro-CT such as 6 specimens from the total 25 lyophilized ones. This gives a percentage of success of 67% for Fixation and CPD and 76% for Lyophilization. In Figure 3.1 can be observed collapsed *M. galloprovincialis* specimens, a fixated and CPD pupa and adult insect (A and B respectively), the figure 3.1 C shows a successful fixation on a *M galloprovincialis* pupa specimen. It is important to refer that the majority of the collapsed lyophilized insects were pupae of *A. syriacus* (As) and that was not possible to try the lyophilization process on *P. perroudi* (Pp) specimens, such as the fixation and CPD process on *A. griseus* (Ag) specimens, because the last larvae died before moulting.

*Figure 3.1: <u>M. galloprovincialis</u> specimens examples of the aspect of collapsed fixated and CPD pupa (A) and an adult insect (B) and the aspect of a successful fixated and CPD pupa (C) (Author's original).*

## 3.2 SEM results

As explained in the methodology chapters, some preliminary tests took place with insects that have not been subject of any previous treatments and that have been photographed as well. In the tables that will be presented (Tables 3.2 to 3.5), are expressed the results of the measurements of all the spiracles of all the insects that were photographed by the SEM technician, regardless of their previous treatment. Notice that, not all the prepared insects were imaged (in appendix III can be found the information of all the specimens sent to SEM) and that the ones that have been, may have not been measured if the images were not clear or if the spiracle was somehow covered (see Figure 3.2, A and B, for examples).

While analysing the photographed spiracles, it came clear some differences concerning essentially the amount of bristles covering the spiracle entrance as well as the shape of the spiracle itself, depending on the insect species and stage of development, and the total number of spiracles.

From the observation of the SEM imaged specimens, a total of 199 spiracles have been measured. Were observed 7 pairs of spiracles in both *M. galloprovincialis* and *A. syriacus* insects, and 8 pairs in *A. griseus* insects, being the first pair (numbered as 1-14 and 1-16, respectively) correspondent with the larger spiracles, and therefore named as "major spiracles".

In Figure 3.3 A is shown a lateral view of a *M. galloprovincialis* where three abdominal spiracles can be observed; Figure 3.3 B shows the major spiracle (msp), corresponding to one of the first pair of spiracles and an evidently smaller one abdominal spiracle. In Figure 3.4 can be observed, more closely, the main aspect of the bristles coverage of a *M. galloprovincialis* pupae's spiracle (A) and an adult's spiracle (B).
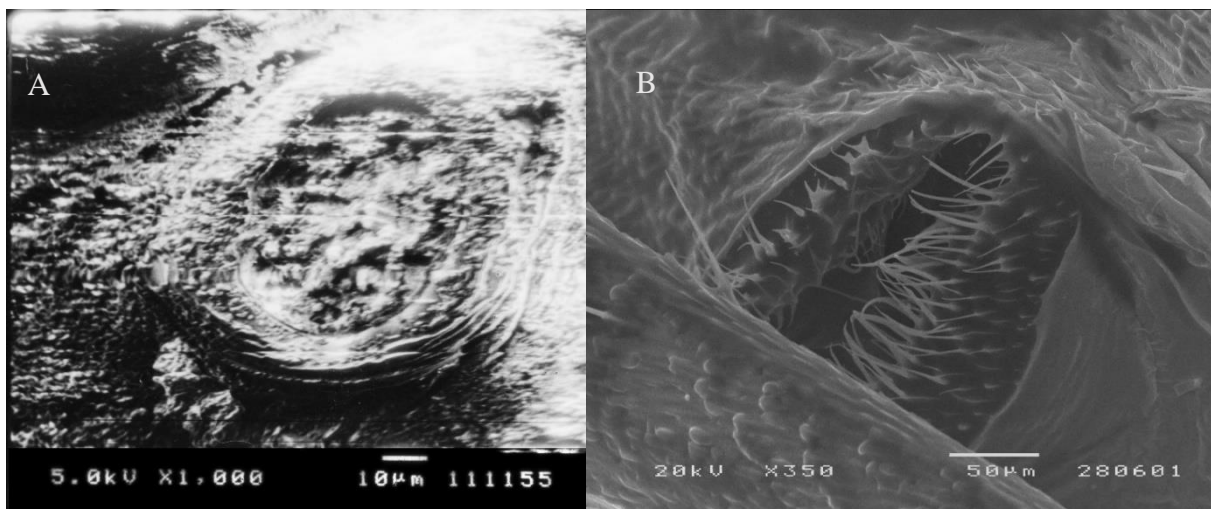


*Figure 3.2: Examples of not measured spiracles, A – an unclear image of a preliminary test on a P. perroudi shot at Instituto Egas Moniz, B – a covered up M. galloprovincialis' spiracle, (Autor's original).*
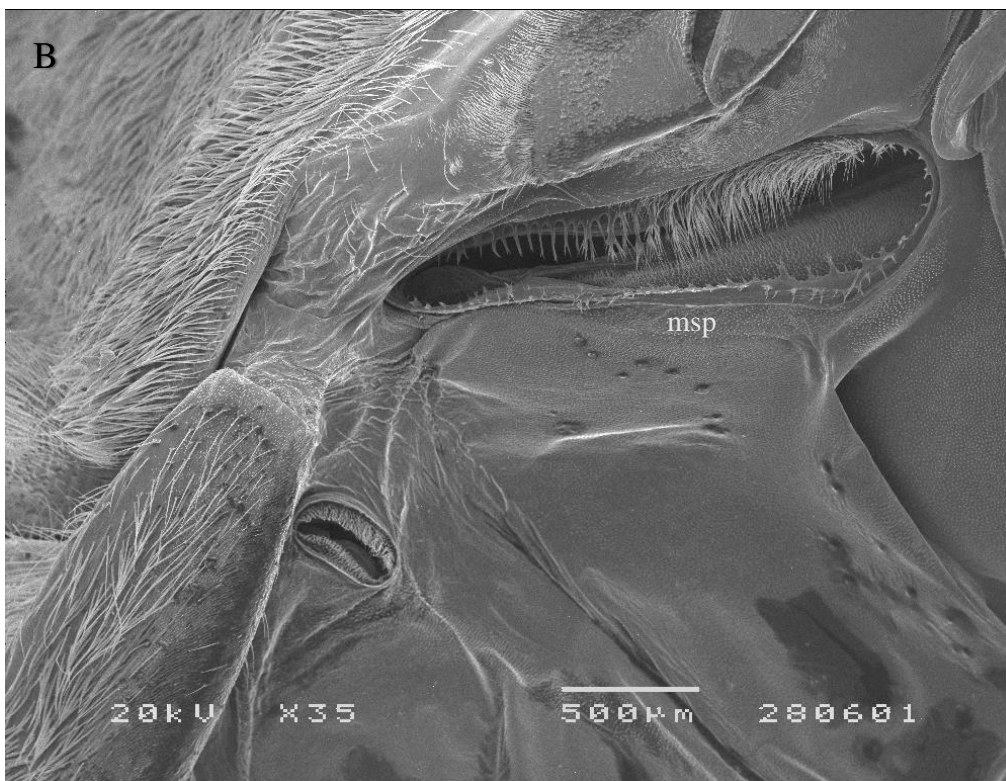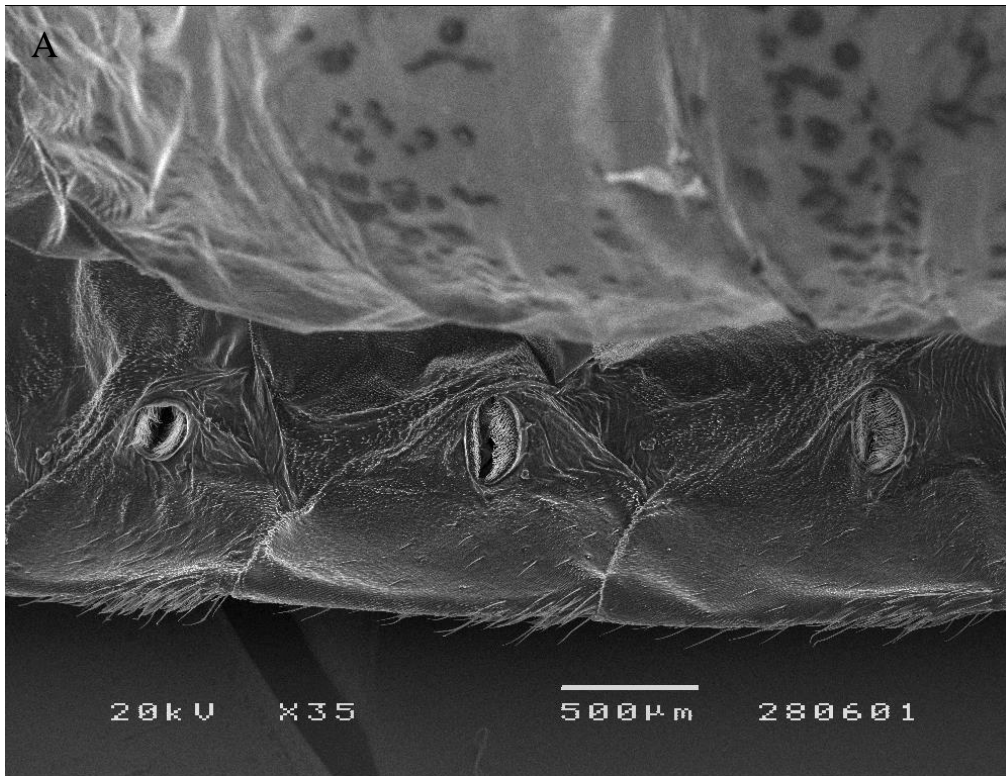
*Figure 3.3: Spiracles of a <u>M. galloprovincialis</u> insect; A- lateral view of the abdominal spiracles, B- major spiracle (msp) size compared to other abdominal spiracle, (Author's original)*
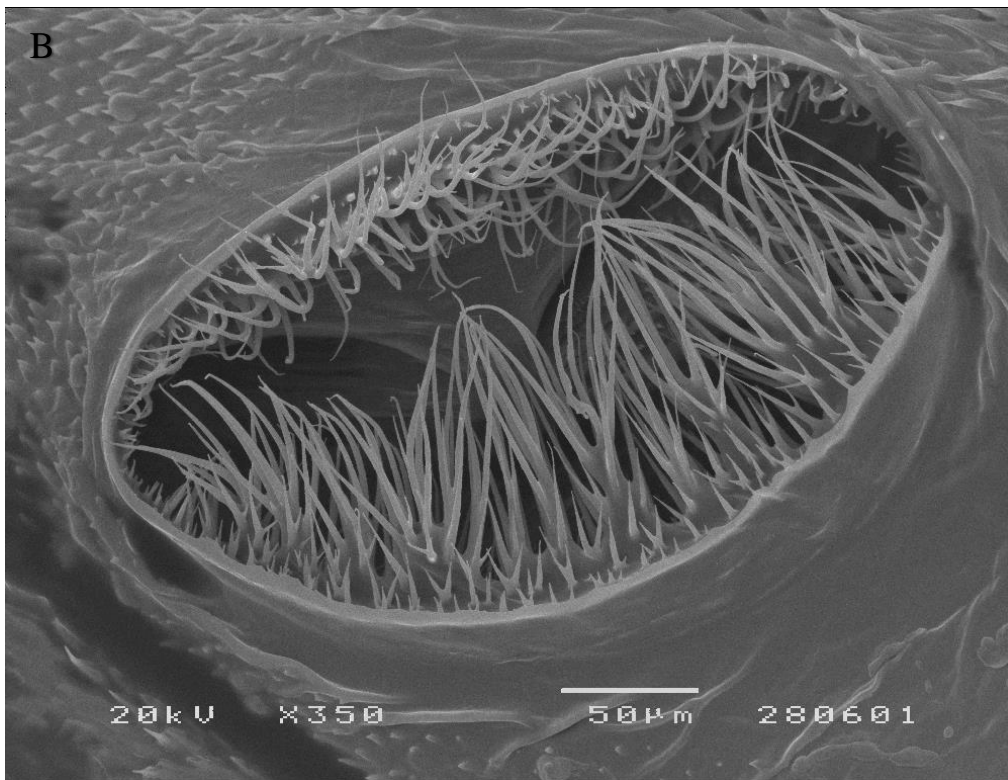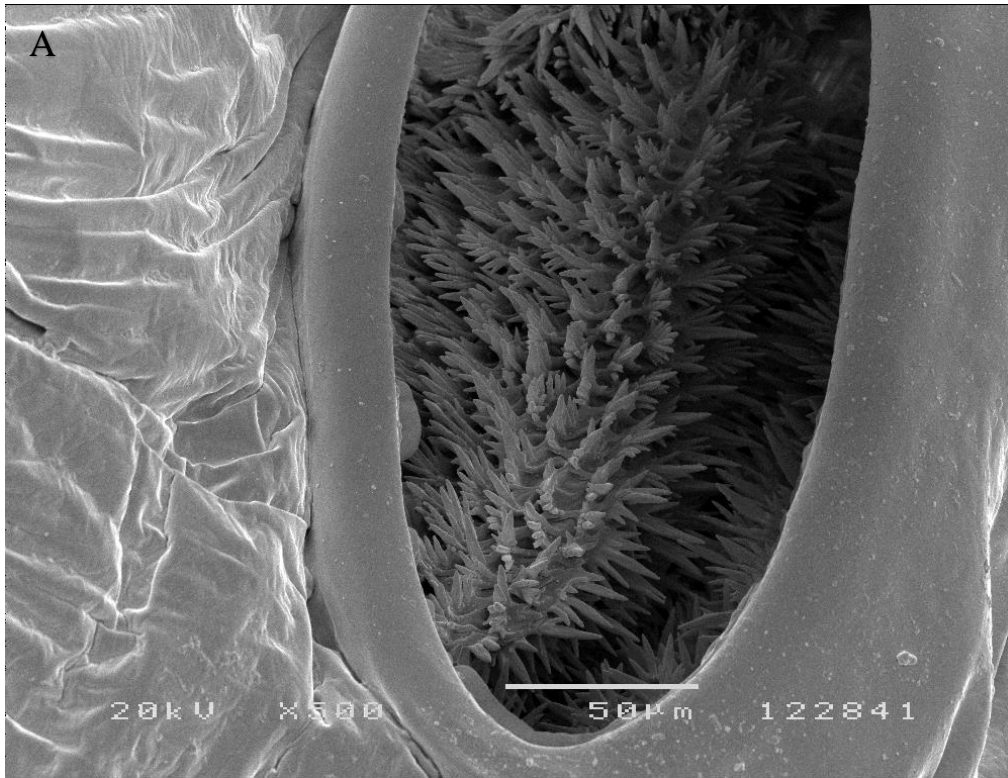
*Figure 3.4: Close up view of the bristles of a <u>M. galloprovincialis</u>, A- pupa spiracle and B- an adult spiracle, (Author's original).*

C

25kV    X750         10μm    280601
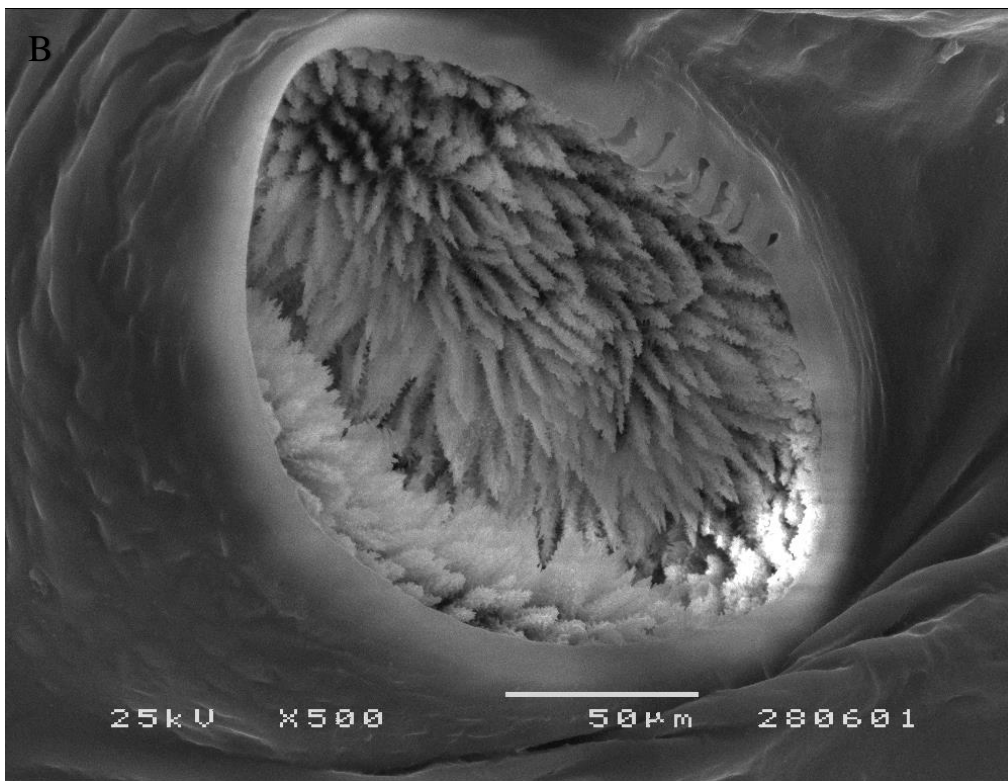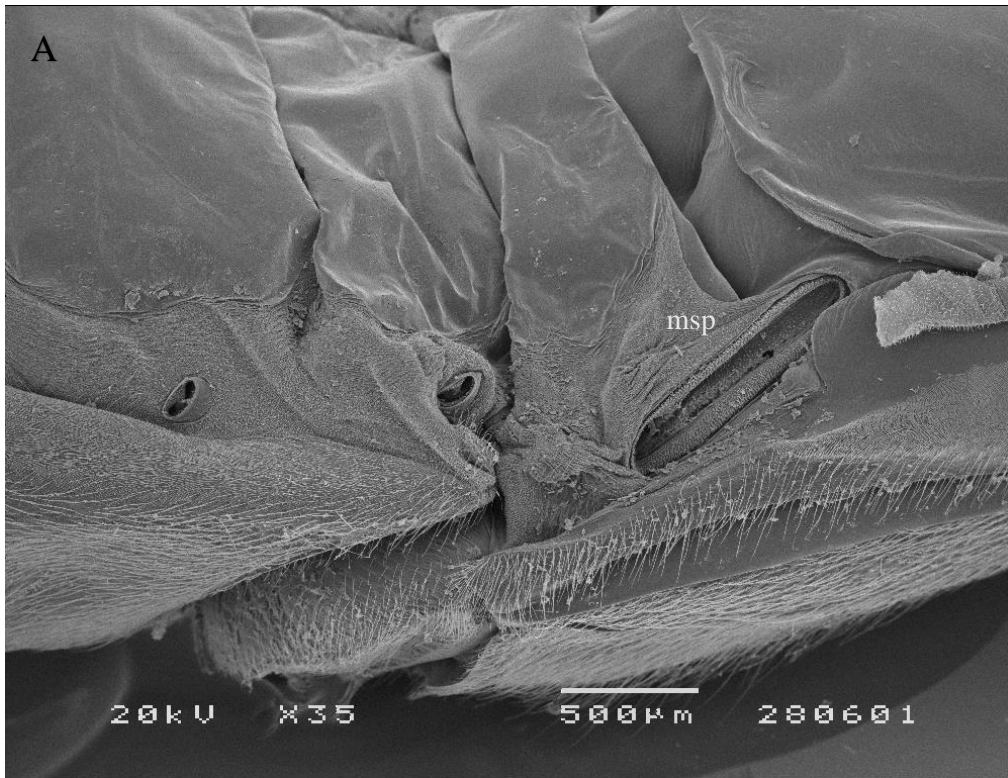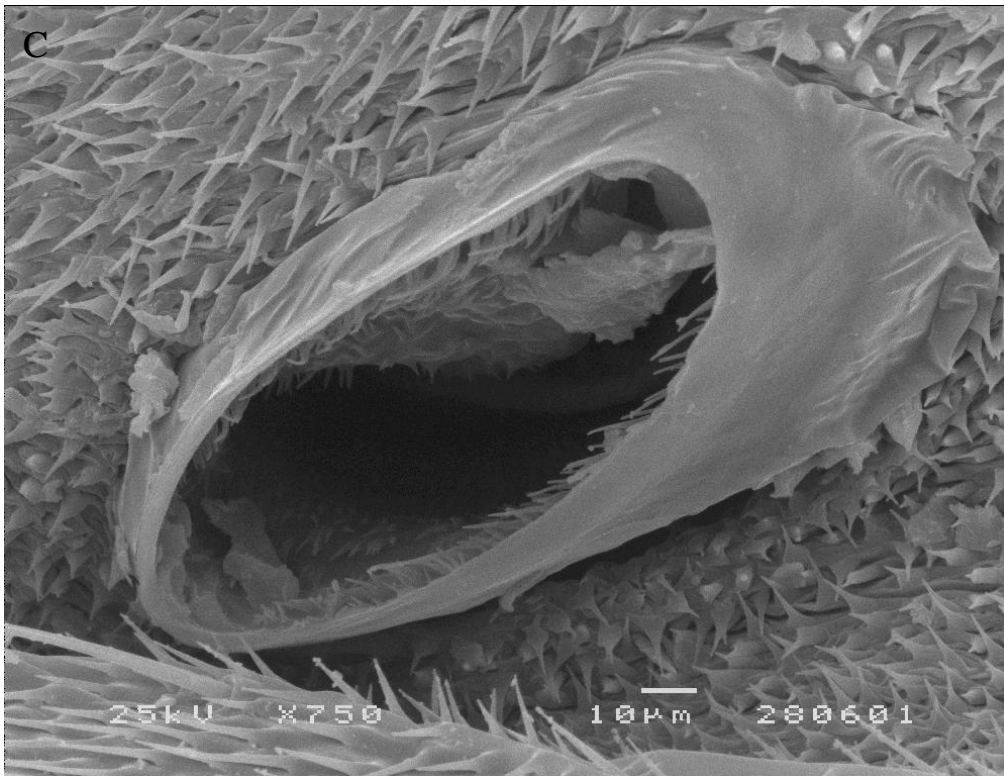
*Figure 3.5: Spiracles of A. syriacus, A- major spiracle (msp) size compare to other abdominal spiracles, B- spiracle of pupa, C- spiracle of an adult insect, (Author's original).*



20kV    X750         10μm    122839
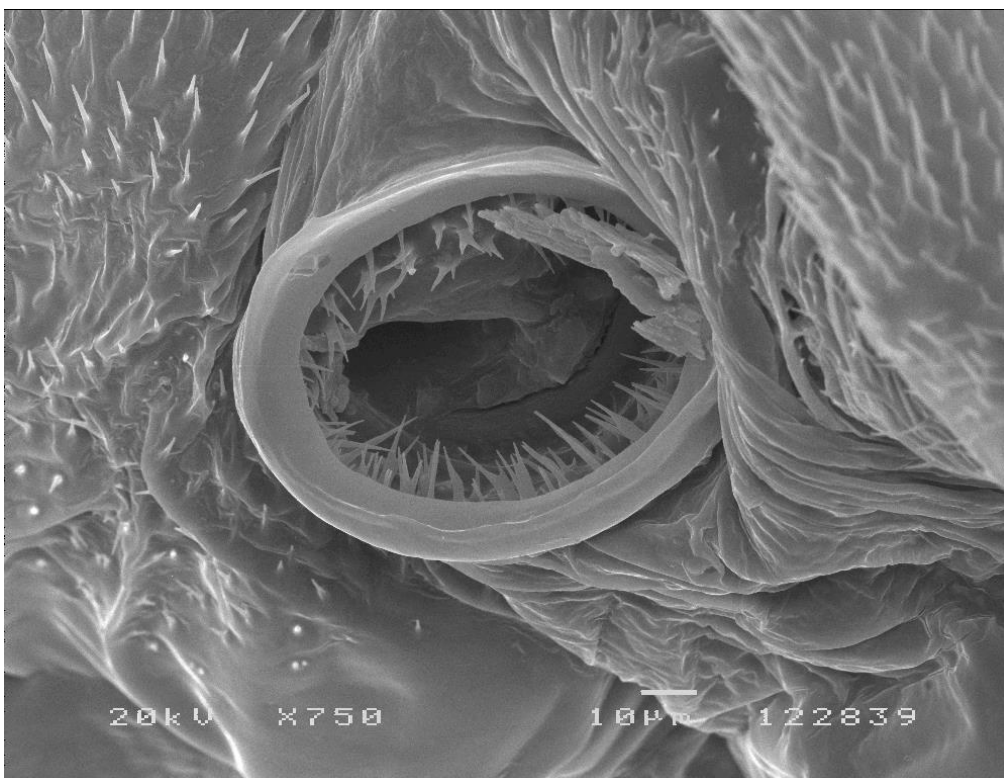
*Figure 3.6: Spiracle of an adult P. perroudi insect, (Author's original).*
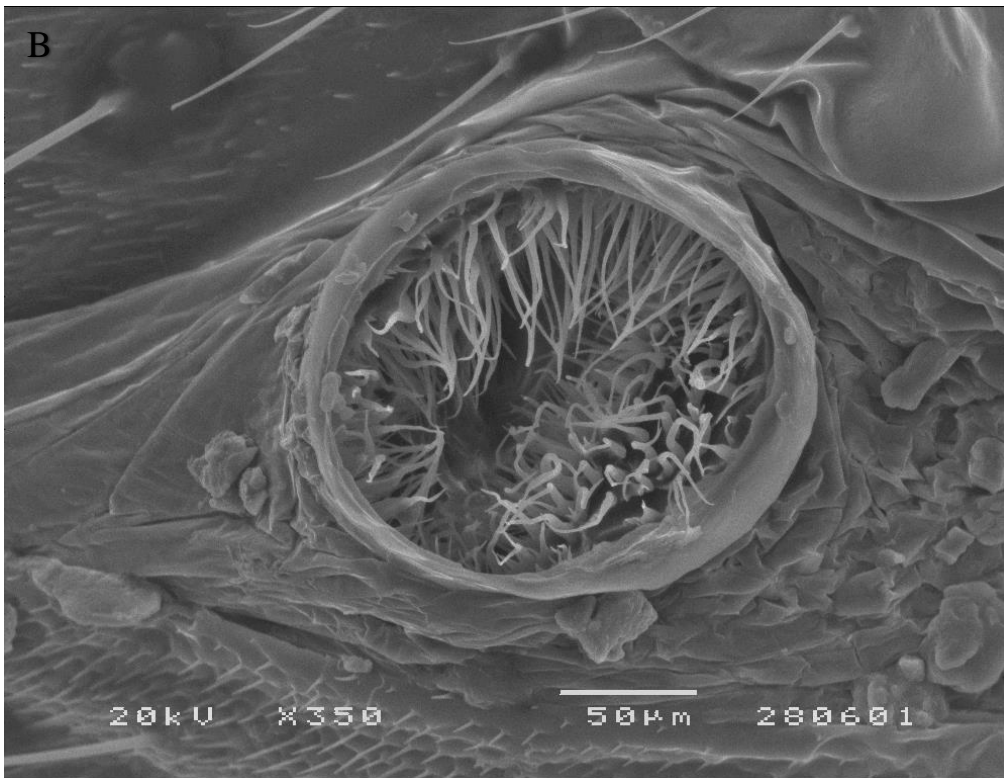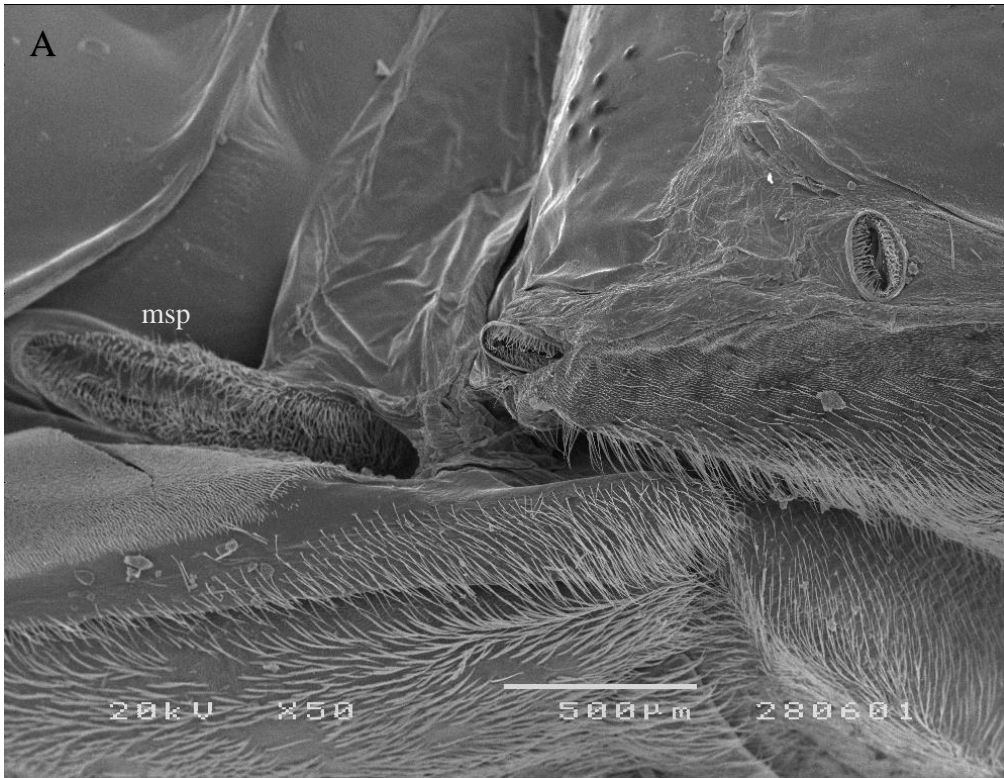
*Figure 3.7: Spiracles of an adult A. griseus, A- major spiracle (msp) size compare to other abdominal spiracle, B- bristles close up view, (Author's original).*

In Figures 3.5 A and 3.7 A it can be seen the different size of the major spiracles compared to the other abdominal spiracles in *A. syriacus* and *A. griseus* specimens as well as the aspect of the bristle's coverage (Figure 3.5 B and C and 3.7 B).

The Tables shows the obtained mean values for the area, circularity and percentage of open area of the measured spiracles; "n" is the number of spiracles that were able to be measure in each insect, which correspond to the number of observations used in the calculations of the mean values. It was calculated the mean values for each insect as well as the mean values for all the spiracles of the same species (referred as Total) and the mean values for the pair of major spiracles and the other pairs separately (spiracles 2-13 in case of Mg and As specimens and 2-15 for Ag specimens). The ID codes marked with '∘' correspond to the insects that had its major spiracles measured, for example, Mg0033 ∘ (Table 3.2), As0005 ∘ (Table 3.3) and Ag0032 ∘ (Table 3.4). Also remember that the different numerations of the specimens stand for the different treatment processes of the samples.

Unfortunately, was not possible to obtain much data about *P. perroudi* spiracles but in Figure 3.6 can be seen the main aspect of an adult spiracle and Table 3.5 presents the mean values obtained from the measurements made from the best 4 images obtained from SEM.

*Table 3.2: Mean values obtained from the measurements of <u>M. galloprovincialis</u>' spiracles.*

| ID | n | Area (mm$^2$) | Circularity | Open Area (%) |
|---|---|---|---|---|
| Mg001 | 9 | 0.0441 | 0.92 | 19.82 |
| Mg002 | 6 | 0.0551 | 0.86 | 12.20 |
| Mg003 | 3 | 0.0417 | 0.95 | 15.97 |
| Mg004 | 8 | 0.0479 | 0.87 | 14.27 |
| Mg005 | 5 | 0.0373 | 0.91 | 22.48 |
| Mg0032 | 11 | 0.0346 | 0.87 | 13.77 |
| Mg0033 ∘ | 11 | 0.1587 | 0.85 | 18.05 |
| Mg0034 | 9 | 0.0317 | 0.89 | 21.82 |
| Mg0035 | 4 | 0.0455 | 0.91 | 29.05 |
| Total | 66 | 0.0608 | 0.89 | 18.01 |
| major spiracles | 2 | 0.6102 | 0.61 | 33.66 |
| spiracles 2-13 | 64 | 0.0437 | 0.89 | 17.52 |
| | | | | |
| **ID** | **n** | **Area (mm$^2$)** | **Circularity** | **Open Area (%)** |
| Mg P001 | 9 | 0.0247 | 0.78 | 3.13 |

*Table 3.3: Mean values obtained from the measurements of A. syriacus' spiracles.*

| ID | n | Area (mm²) | Circularity | Open Area (%) |
|---|---|---|---|---|
| As001 | 6 | 0.0083 | 0.77 | 66.79 |
| As0002 ∘ | 11 | 0.0450 | 0.65 | 67.56 |
| As0004 ∘ | 7 | 0.0394 | 0.56 | 85.64 |
| As0005 ∘ | 10 | 0.0465 | 0.69 | 80.90 |
| As0030 ∘ | 5 | 0.1879 | 0.50 | 84.97 |
| As0032 | 9 | 0.0053 | 0.71 | 86.20 |
| As0034 | 5 | 0.0035 | 0.61 | 97.35 |
| As0035 | 6 | 0.0051 | 0.51 | 95.14 |
| As0036 ∘ | 9 | 0.0170 | 0.64 | 92.48 |
| As0037 ∘ | 7 | 0.0368 | 0.61 | 75.50 |
| Total | 75 | 0.0364 | 0.64 | 82.29 |
| major spiracles | 10 | 0.2279 | 0.42 | 75.68 |
| spiracles 2-13 | 65 | 0.0070 | 0.67 | 83.30 |

| ID | n | Area (mm²) | Circularity | Open Area (%) |
|---|---|---|---|---|
| As P0003 | 12 | 0.0246 | 0.86 | 1.14 |
| As P0004 | 13 | 0.0172 | 0.83 | 0.38 |
| Total | 25 | 0.0208 | 0.84 | 0.75 |

*Table 3.4: Mean values obtained from the measurements of A. griseus' spiracles.*

| ID | n | Area (mm²) | Circularity | Open Area (%) |
|---|---|---|---|---|
| Ag002 | 5 | 0.0247 | 0.89 | 39.38 |
| Ag0030 | 5 | 0.0226 | 0.74 | 33.15 |
| Ag0032 ∘ | 12 | 0.0448 | 0.78 | 15.17 |
| Total | 22 | 0.0352 | 0.79 | 24.76 |
| major spiracles | 2 | 0.1789 | 0.38 | 6.16 |
| spiracles 2 - 15 | 20 | 0.0208 | 0.84 | 26.62 |

*Table 3.5: Mean values obtained from the measurements of P. perroudi adult's spiracles.*

| ID | n | Area (mm²) | Circularity | Open Area (%) |
|---|---|---|---|---|
| Pp001 | 4 | 0.0022 | 0.96 | 72.55 |

A better way to visualize the main differences between the measured features is to represent them in a graphics. In the next figures it can be seen the box plots which present mean, median, minimum, maximum, 25% and 50% quantile values, correspondent to the distribution of the percentages of Open Area and Circularity. For a better understanding, the percentages for pupa and for adult specimens were presented in different graphics, Figures 3.8 and 3.9 respectively.

Figure 3.10 presents the box plots concerning the distribution of the circularity values for adults of the four species and *M. galloprovincialis* and *A. syriacus* pupae. For *P. perroudi* (Pp) the overlapping values, are 0.97, 0.96, 0.95, from top to bottom.
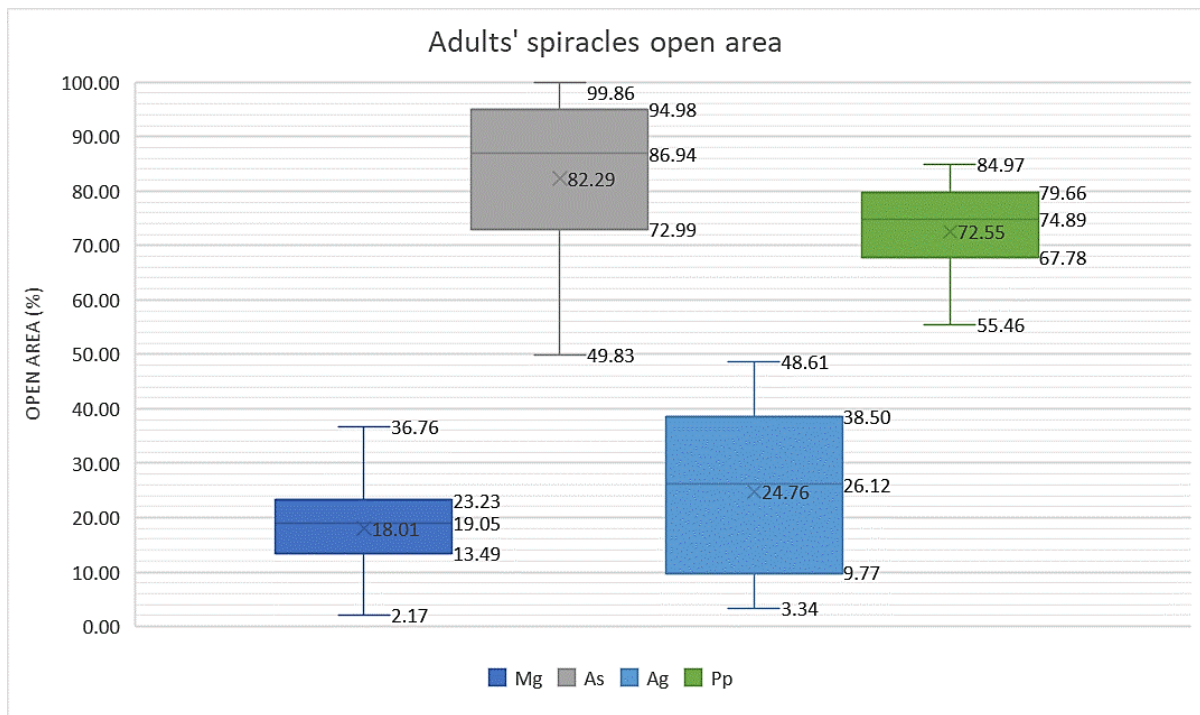


*Figure 3.8: Box-plot graphic for the distribution of the open area percentage of the four species' adults, M. galloprovincialis (Mg), A. syriacus (As), A. grisues (Ag) and P. perroudi (Pp).*
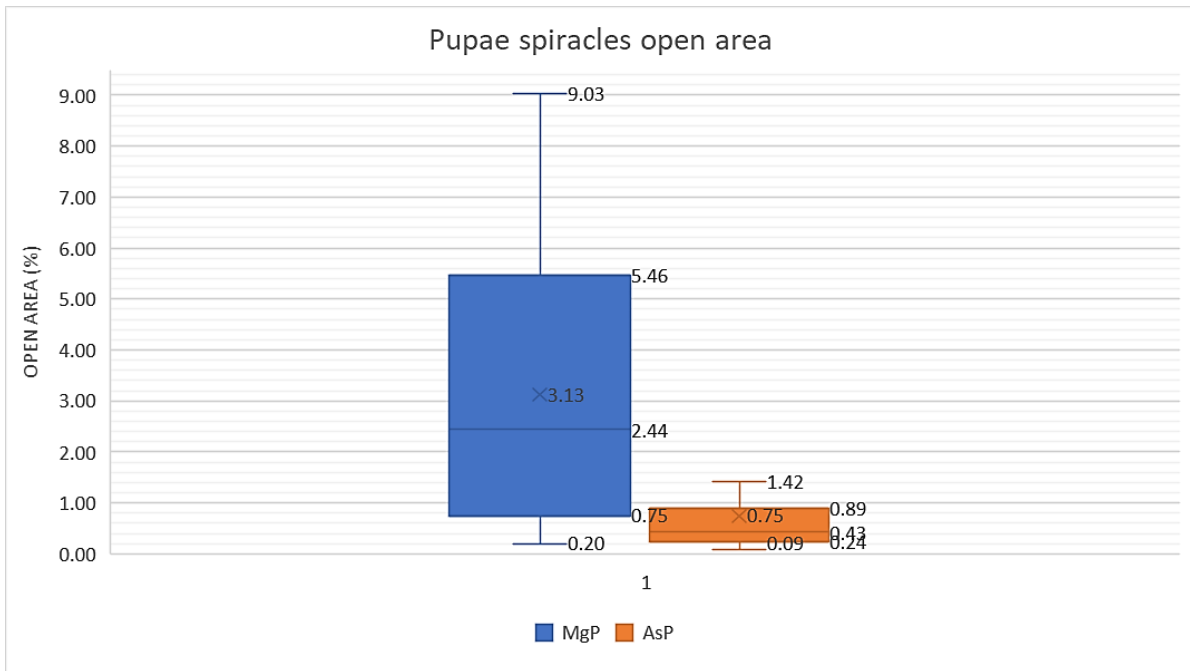
*Figure 3.9: Box-plot graphic for the distribution of the open area percentage of M. galloprovincialis (MgP) and A. syriacus (AsP) pupae.*
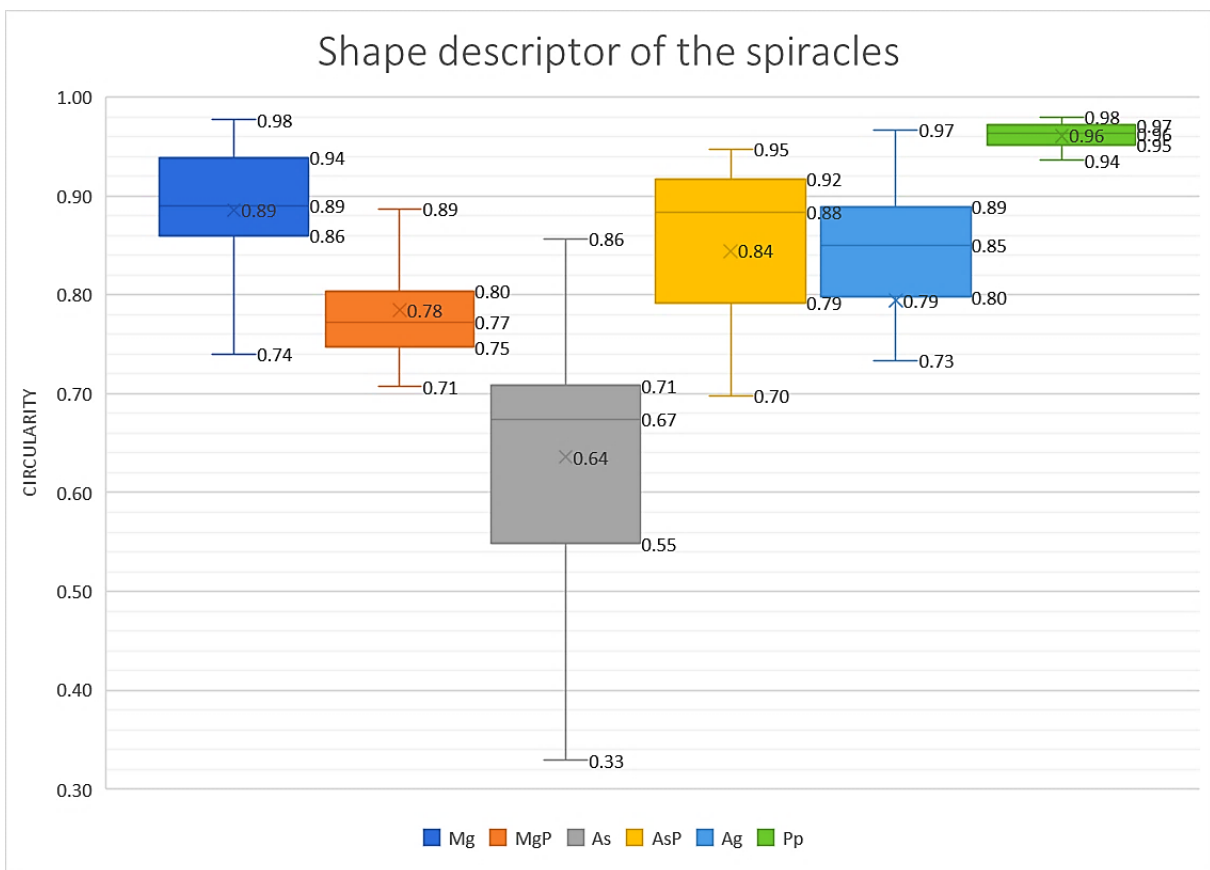


*Figure 3.10: Distribution of the circularity values obtained for the measured spiracles of M. galloprovincialis (Mg), A. syriacus (As), A. grisues (Ag) and P. perroudi (Pp) adults and M. galloprovincialis (MgP) and A. syriacus (AsP) pupae.*

## 3.3   Micro-CT results

The raw images obtained in the acquisition step of the Micro-CT scan are digital radiographies, (Figure 3.11 A). After the reconstruction step a 2D transversal cross-section can already be observed, showing the internal anatomy. Figure 3.11 B shows a *M. galloprovincialis* pupa 2D cross-section in which some anatomic features of the abdomen can be seen such as

Figure 3.12 is an example of what can go wrong during the acquisition step; a non-treated insect that did not endure the scanning, and collapsed (A), and a lyophilized insect that despite looking well preserved, the 2D transverse cross-section images presents artefacts similar to wood grown rings (B).

Figures 3.13 A and B shows a virtual volume of a *M. galloprovincialis* adult insect as a result of the primary segmentation where the Eppendorf tube (epf) have been practically removed.

*Figure 3.11: M. galloprovincialis fixated and CPD pupa A- raw Micro-CT image, B- 2D transverse abdominal cross-section showing: trachea ramifications - trc, legs - lg, antennae - ant, wings - wg, posterior digestive system/intestine - pDS, and the 10 millimeter diameter Eppendorf tube – epf, (Author's original).*
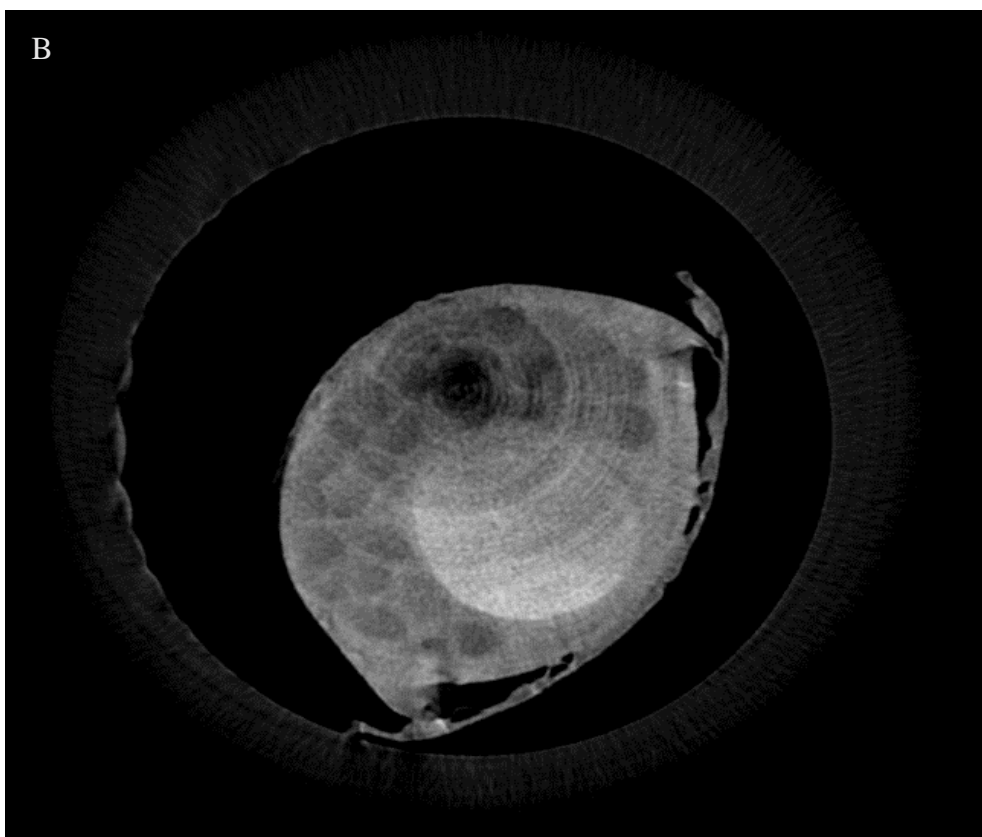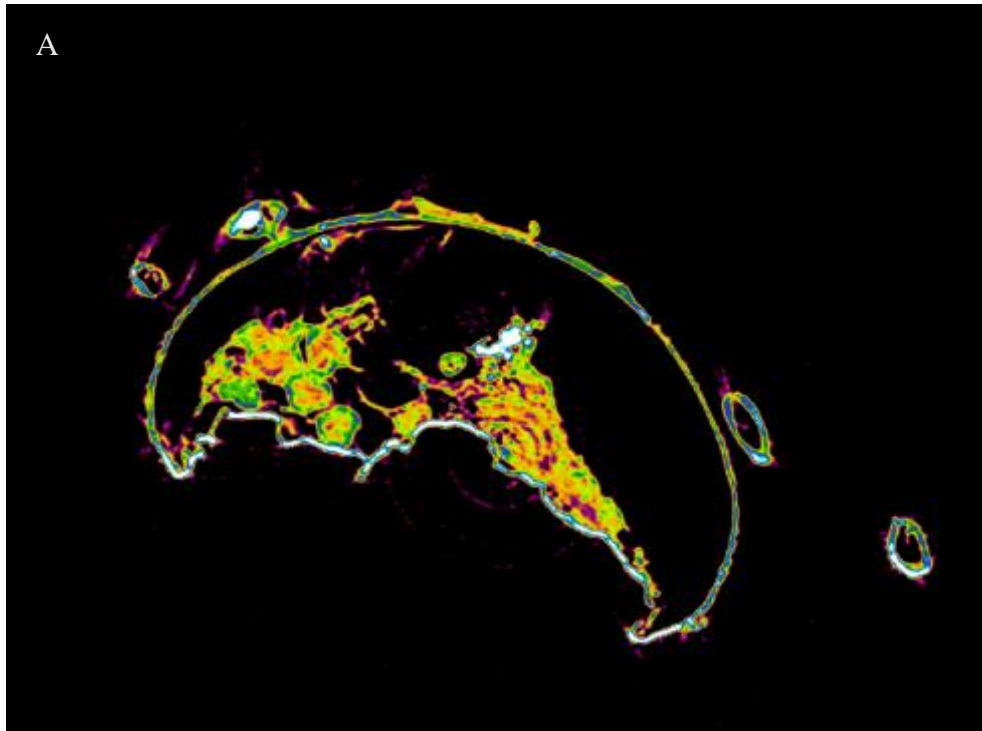
*Figure 3.12: 2D transverse cross-sections A – Not treated A. griseus adult insect collapsed during Micro-CT scan, B – Lyophilized A. syriacus adult insect with artefacts formed during the Micro-CT scan, (Author's original).*

*Figure 3.13: Adult M. galloprovincialis insects virtual volume viewing on CTVox software from BRUKER®, A – general view of the sample, B - close up ventral view, (Author's original).*

With CTVox software is possible to move the virtual volume to observe different aspects of the internal anatomy while maintaining a sense of depth and spatial arrangement of the organs. Figures 3.14 and 3.15 shows different cross-sections views of an adult *M. galloprovincialis* virtual volume. Also were created some videos with this tool to show the complexity of the insect internal anatomy [ii].

---

[ii] The videos, as complement of the thesis, can be accessed on
http://web.tecnico.ulisboa.pt/ist13225/DISSERTACAOANALEALMATERIALCOMPLEMENTAR.pptx.
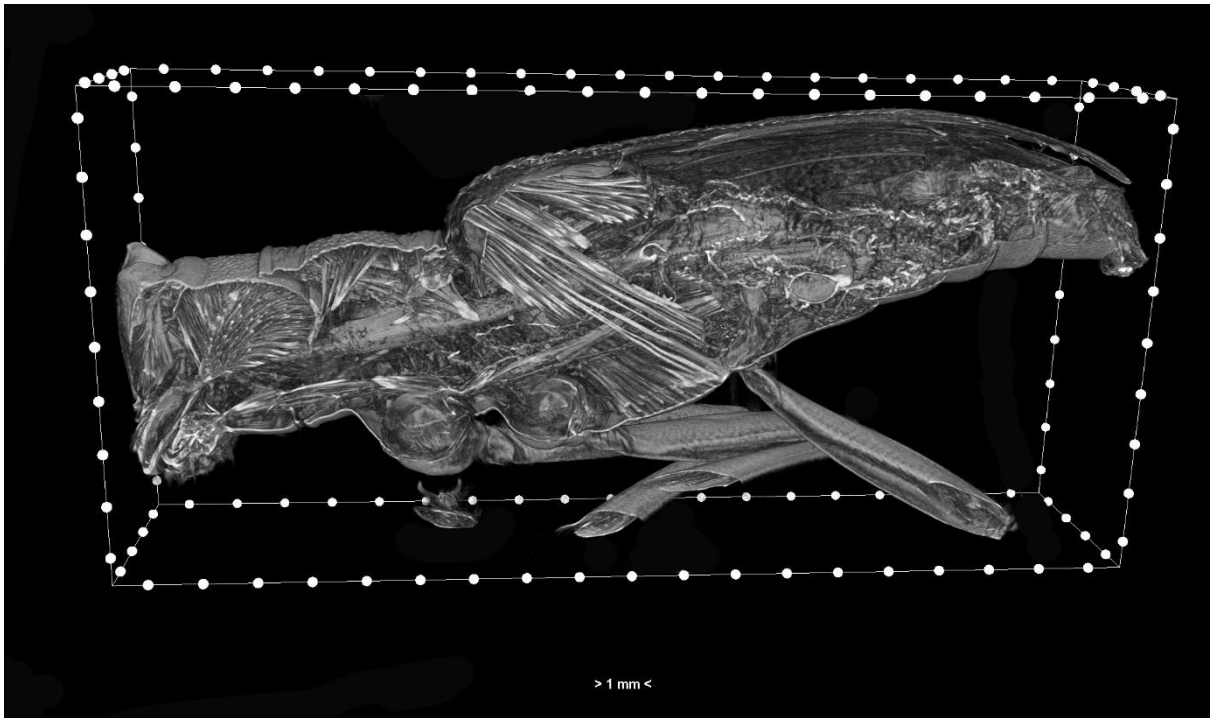
*Figure 3.14: Adult <u>M. galloprovincialis</u> sagittal section inside a scale box of CTVox software (Author's original).*
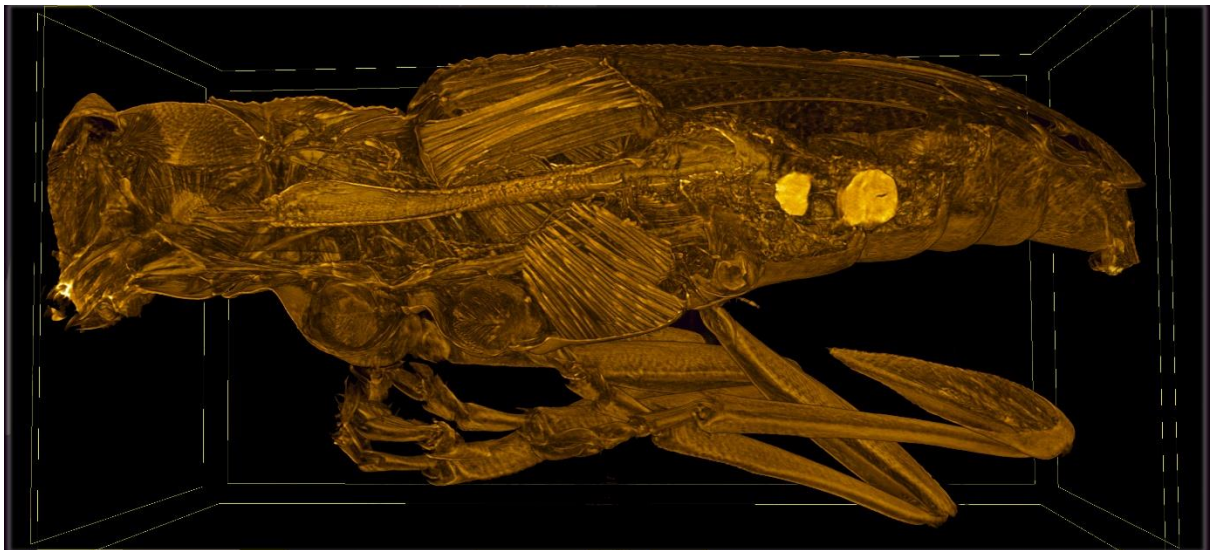


*Figure 3.15: Adult <u>M. galloprovincialis</u> sagittal section enhancing a high density organ (Author´s original)*

### 3.3.1 Multiple ROI

The Multiple ROI shapes approach for segmentation of the main tracheal trunks using Image type ROIs (procedure described in sub-chapter 2.1.1) was a new method try-out for this type of samples. Despite the fact that it was possible to create the masks needed for several 2D cross-sections of a *M. galloprovincialis* pupa, unfortunately, we were not able to load the masks into the CTAn software as Image ROIs and consequently was not possible to create a virtual volume of the tracheal trunks as had been predicted.

### 3.3.2 Tracheal Volume Estimation

From the area measures of the main identified tracheal trunks, the volume of the ramifications in the specimens' head, thorax, abdomen has been calculated and the estimated total volume was also calculated as the sum of the volume of the four head and thorax ramifications plus the volume of the two abdominal ramifications. The values are presented in Table 3.6 below as well as the mean diameter of the measured ramifications.

*Table 3.6: Tracheal Volume Estimation and mean Trachea Diameter of one male (M), one female (F), one pupa (P) of M. galloprovincialis (Mg), one adult A. syriacus (As) and one male (M), one female (F) A. griseus (Ag), (Length and Diameter presented in millimeter (mm) and Volume presented in cubic millimeter (mm³)).*

| Specimen | Length (mm) | | | | Tracheal Volumes (mm³) | | | | Trachea Diameter (mm) |
|---|---|---|---|---|---|---|---|---|---|
| | Body | Head | Thorax | Abdomen | Head | Thorax | Abdomen | Total | |
| Mg P | 14.38 | 3.584 | 5.681 | 5.115 | 0.955 | 0.157 | 0.143 | 1.256 | 0.218 |
| Mg (M) | 19.30 | 3.839 | 5.616 | 9.841 | 0.735 | 1.111 | 0.517 | 2.363 | 0.301 |
| Mg (F) | 17.54 | 3.013 | 5.004 | 9.521 | 0.363 | 1.209 | 1.247 | 2.819 | 0.350 |
| As | 21.40 | 2.964 | 7.380 | 11.06 | 0.408 | 1.377 | 0.615 | 2.400 | 0.298 |
| Ag (M) | 9.046 | 1.426 | 3.033 | 4.586 | 0.028 | 0.047 | 0.080 | 0.156 | 0.103 |
| Ag (F) | 9.776 | 1.679 | 4.206 | 3.890 | 0.024 | 0.077 | 0.084 | 0.185 | 0.092 |

# 4 Discussion

## 4.1 Preamble

Primarily, it is important to remember that at the very first beginning of the work, it was purposed to observe both the tracheal system and the spiracles in the same specimen, and that was the main reason for the search for a stabilization process that would allow the specimens to endure both analyses. In order to do so, the experimental procedure was thought as Fixation and Critical Point Drying, followed by the Micro-CT scanning, then isolation of the specimens' abdomen so it could fit in the sample holder and be coated with gold to be properly photographed in SEM.

While learning about the techniques, and during the preliminary tests, it became clear that such thing would not be achievable for various reasons. One of the main obstacles was the fact that the SE Microscope and the Micro-CT scan were stationed at different laboratories, one in the Science Faculty and the other in Technical Institute (IST-UL), such as the technicians responsible for their handling. Also, various consulted papers suggested the use of fresh collected, killed and preserved specimens for a successful fixation and scanning [28] and by comparing the SEM and Micro-CT preliminary images to the ones obtained with the first fixated specimens, has confirmed a better outcome when fresh specimens were used. Although it was possible to measure several spiracles of non-treated insects it is important to refer that the specimens used in SEM and Micro-CT preliminary tests were the ones that looked better preserved. The spiracles being placed superficially in the body, make its observation easier; if the coating is done right, it is more likely to be able to observe some of them, even if the tissues were wrinkled, due to the range of movement that the sample holder offers. Even so, when looking for the Micro-CT scans, the scenario was different. The internal structures of the non-treated scanned specimens were, in majority, shrunken and indistinguishable as presented in Figure 3.12 A.

To apply fixation procedures to fresh insects after preliminary testing, we had to wait about five months for the larvae to grow and moult into pupae and adults, so the fixation events could happen. The fixation itself is a slow process, with a duration of about one week from submerging the specimens into the fixative until the end of the dehydration process. The first fixation event occurred in middle April and the last one occurred in late July. Critical Point drying is a little faster, but still takes about 24 to 48 hours to be completed once that our species are considered large ones. Also, this step of the process was performed in a third different laboratory (FCUL, Rua da Escola Politécnica) and the technician responsible processes the samples only once a week.

Due to all the mentioned reasons, following the initial experimental procedure would implicate that the specimens were transported from one laboratory to another several times and that the analyses would keep being more and more delayed. So, it was decided to perform the fixation and critical point drying as insects were grown, then the specimens were observed in an optical microscope and divided between SEM and Micro-CT as already explained during the Methodology chapter.

While observing the insects in the optical microscope, was noticed the existence of a pair of larger spiracles than the abdominal ones, that would not be studied if we continued to isolate the abdomen for SEM, as initially planned to do. So, it was decided to remove only the appendages, legs, elytra, antennae and wings, as referred in the Fixation and Critical Point protocol (chapter 2.1.1).

Even with these changes in the experimental procedure, the data acquisitions were still delayed. In an attempt to overcome the long-lasting process of chemical fixation and critical point drying, was suggested by Professor A. Cristina Figueiredo, to try to lyophilize a few of our specimens. Even though there have not been found evidence of success in stabilization of organisms such as insects, the process is less time consuming, has fewer laboratory resources needs and has been used in a vast type of living organisms such as bacteria and fungi. For these reasons we thought it would be worth a try.

The time spent solving all the unexpected methodological problems forced to terminate the data acquisition before achieving the repetitions initially planned and required for a proper statistical assessment or a mathematic based comparison between different methods. Therefore, the results presented are only based in mean values and percentages. Even though, in the next sub-chapters, will be discussed both our conclusion based in the obtained results and the main difficulties faced during the different procedures, and finally will be presented future perspectives.

## 4.2    Fixation and CPD versus Lyophilization

As already mentioned, lyophilization appeared as an alternative for the long-lasting fixation process. As shown in the results, the success of the two procedures is not that different, 76% against 67% respectively. However, the number of specimens stabilized with these procedures is not the same, and it was not possible to perform both techniques at specimens of the four species because the number of larvae was not the same for the four studies species and also because some of them died before moulting. Also, it is obvious that something went wrong during the *A. syriacus* pupae lyophilization since all collapsed. For that reason, further experiments would be needed in order to understand if this was an occasional event or what factors (pressure and temperature settings or duration of the process) could have determine this outcome.

Several papers and experimental protocols refer that both Glutaraldehyde and Osmium tetroxide or Hexamethyldisilazane fixation have satisfactory outcomes in stabilization of samples for SEM and Micro-CT. Even more, referred that osmium can act as a contrast agent for the observation of some internal structures [35,48].

The insects were submerged still alive in the fixative as an attempt to improve the impregnation of the fixative agent into the internal organs once that the insect would be breathing it in. Also, to improve the diffusion through the insect body, the fixation took place at room temperature contrary of at low temperatures as stablished in the original protocol [43].

In what concerns the fixation outcomes, it seems that *M. galloprovincialis* pupae bear quite well the treatment once that only a few ones collapsed, compared with the adult insects of the same species. For the other specimens of the non-vector species, it seems that the procedure is also a success, although again, we are not comparing samples with the same number of individuals.

A reason for the failures of fixation may be the fact that some samples, after dehydrated, had to wait several days (sometimes even weeks) to be critical point dried. As the insects grew, when available about 5 to 10 specimens, being 10/14 days old pupae or newly formed adults, they were fixated. Fixation must be a continuous process from the moment the insect is submerged until the last acetone substitution for dehydration. Only then, the specimens can be maintained in waiting for CPD, stored at a fridge, to slow down the evaporation of the acetone. But even so, acetone keeps evaporating, and if no more is added, the specimen dry out abruptly, consequently the tissues may collapse and shrink.

Even if fixation seemed successful and the specimens arrived stabilized to CPD, sometimes the specimens do not bear the pressure inside the CPD chamber and collapse or burst from inside out (as the insects shown in figures 3.1 A and B) Despite the limitations, because of its applicability to virtually all type of specimens, it remains the standard method [35]. The ideal scenario would be that the CPD takes place at the same place and within few days after the fixation to decrease the probability of a failure.

## 4.3 SEM results

While learning about the PWN, the insect vector and the interaction between them, initially was though that *M. galloprovincialis* spiracles would have a low bristles coverage comparatively with the other species and that would be the reason why their spiracles are the entrance into the insect body for the nematode but the obtained percentages for the open area offers a new perspective.

Measuring the area not covered by bristles and calculate the percentage of the total area at which it corresponds, was the best way found to quantify the visible differences on thsyre bristle coverage. This means that as the percentage of the open area decreased, the coverage of bristles increased.

Adult *M. galloprovincialis* insects have a mean percentage of open area of 18.01%, while the adults of the other three species have higher mean percentages of open area: 24.76% for *A. griseus*, 72.55% for *P. perroudi* and 82.29% for *A. syriacus* (review tables 3.2 to 3.5). As it can be notice, *M. galloprovincialis*' adults have the lowest percentage of open area, which means that almost all the spiracle is covered with bristles. However, for insect-vector pupae spiracles, the mean percentage of open area is 3.13%, even lower than the one of the adults but still higher when compared with *A. syriacus*' pupae (0.75%) which means that their spiracles are abundantly covered up with bristles.

While the non-vector species, have lower bristles coverage, the insect-vector has only a small area not covered by them. This can imply that the bristles should help the nematode to tangle itself and crawl into the trachea while provide a moisture environment that also favours the nematode survival and movement. On the other hand, the bristles coverage of the pupae may be so dense that in this stage of the insects' development it can work like an obstacle for the nematode entrance. This may be the reason why the PWN enter the spiracles only when the newly adult insects are formed.

In what concerns the shape of the spiracles, and looking back to the Circularity values distribution (Figure 3.10), it appears that there are not major differences among *M. galloprovincialis*, *A. syriacus* and *A. griseus* insects, and that these three species have spiracles more round and others more elliptical, being the major spiracles the less round ones (with minor circularity). The exception is *P. perroudi* 's spiracles that have high circularity values, being those practically round. Even so, there is no evidence that the shape of the spiracles may represent an important feature to explain how PWN colonizes the insect-vector, or why it prefers *M. galloprovincialis* over the other species.

The evolutionary purpose for these insect vs nematode interaction is for the nematode to "catch a ride" to a new host tree, and that is itself a reason why the nematode seeks for the adults that are about to emerge and fly way to new areas and new host trees. How it identifies the insect-vector is another question still to be answered.

Our morphological observations seem to indicate that the probability of the three non-vector studied species to become a way of dispersion of the PWN, is a remote one. The species that has a percentage of spiracles' open area nearest to the one of *M. galloprovincialis* is *A. griseus*, but these insects are smaller, less abundant than the vector (review Appendix I and Annex I) and colonizes mostly the branches of the host tree, being less available for the nematode [49].

*Arhopalus*, which has almost the same body length as the insect-vector, is more abundant then *M. galloprovincialis*, but as seen in the pictures and in the open area values, the spiracles are structurally different, having more bristles, something that would be expected since the species belong to different sub-families, *A. syriacus* is a Spondylidinae while the other three species are Lamiinae.

The smaller and less abundant of all is *P. perroudi*. Despite being a Lamiinae, its spiracles are, as well, different from the ones of the insect-vector, being smaller than any of the others. Also, *P. perroudi* colonizes preferentially dying branches and host trees [49]. Conditions that may be not appreciated by the PWN, once it is when the host tree start to languish, that the nematode moult to its dispersal form to get ready to move to a new host tree.

## 4.4 Micro-CT results

Many factors contribute to the success or unsuccess of Micro-CT, thus resulting in discrepancies among studies [50]. Despite the fact that Micro-CT is considered a non-invasive technique for the observation of internal anatomy, it can always provoke structural changes in the samples, after all, the biological samples, as the ones we worked with, have to endure the fixation, dehydration, CPD and the acquisition step which occurs in a low-pressure chamber. Initially were done multiple acquisition with fresh insects [51]. Usually the second acquisition is relatively stable, and the results were acceptable, especially for *M. galloprovincialis* robust mature insects. Also, sometimes during a CT scanning process, the sample moves, either due to its one weight, or the heat caused by the X-ray beam causes alterations in the samples volume, or the source current oscillates, creating artefacts and distortion that unviable the images, making useless several hours of acquisition that have to be repeated.

Some authors refer that specimens preserved in alcohol and scan directly had results somewhat disappointing [26], a fact that we observed in some of the studied insects. Others refer that good results can be obtained either with critical point dried or hexamethyldisilazane treated specimens [28] or fixated and stained with osmium tetroxide [35,48]. However, other authors still defend that structures like the trachea do not appear in CT scans if stained with osmium, defending that trachea ramifications can be accurately imaged only because they are air filled tubes which provide a strong contrast from the surrounding structures [50].

From our observations, we were able to measure tracheal trunks in one lyophilized specimen, in specimens fixated with glutaraldehyde and osmium tetroxide, and critical point dried, and even in not treated specimens, although in this last case it was harder to find the main trachea trunks lengthwise the entire body of the insect. An explanation for the observation in both treated samples may relay in the fact that the solvents, being water or acetone, were removed from the structures, or by critical point or by the lyophilization, living the air filled space that could create the contrast needed to visualize the trachea. Maybe, osmium tetroxide really helps to enhance the contrast facilitating the observation.

As already mentioned in the Methods Approach chapter, when there is a big difference in the contrast among structures, for example if working to individualize bone and muscle, it is possible to almost automatically perform a segmentation, but when the structures have similar densities, as ours, the contrast between them is low, which make the process of segmentation much more time consuming and strongly relied on the skills of the operator.

The Multiple ROI Method is a promising one, with a lot of potential in what regards the decrease of user's analyses time, but we were not able to load our Mask into the CTAn. Errors as "Image too fragmented" or "ROI shape not recognized" were constants, also, while trying to load one mask, the software crashed. We updated the CTAn software, we try to binarize the image at ImageJ instead of doing it in CTAn but unfortunately, we were not able to make it work.

In what concerns the tracheal volumes estimation, it is evident that more data is needed. However, the volume values obtained are consistent with the insects' body length and diameter of the main trunks with the described morphology of the trachea ramifications for Coleoptera insects which suggests that our observations are correct, that we indeed were able to identify the main tracheal trunks.

It can also be observed that the bigger specimens, *A. syriacus* and *M. galloprovincialis*, are the ones with the higher tracheal volumes, which was expectable once that the tracheal system spreads to the entire body to provide oxygen to all the organs. Comparing *M. galloprovincialis'* male and female it appears that exist some differential distribution of the tracheal trunks between the sections measured among the gender. The total tracheal volume is similar between them, while the tracheal volume of the female's abdomen is twice of the males' abdomen, though in the other specimens seems to stand more uniform among the three sections, head, thorax and abdomen. This would be an interesting approach for further analysis.

## 4.5    Future perspectives

Presently, pest management measures are mainly focused in preventing the spread of the PWN by controlling the insect-vector with massive traps and by cutting the infected tress. Better understanding on the inter-relationships between the nematode, its insect-vector and the host pines trees is clearly essential for control of *B. xylophilus*, so further investigation in these matters should be supported. All the work done to adjust the stabilizations processes to our samples and the rest of the methodology for observation an analysis of data, is an asset for further works that may try to visualize the same anatomic features on similar specimens.

Our work comparing the vector species trachea morphology with non-vector species, may offer further understanding about the dependent relationship between *M. galloprovincialis* and the PWN. We have plenty of information in the data obtained from Micro-CT that we were not able to process; new 3D Segmentation and volume analysis tools as VGStudio Max or Amira [44] software may overcome some of the challenges we faced in characterizing the Tracheal System.

It is also very important to integrate all the data already available on the anatomy of the insect, the anatomy of the nematode, the environmental factors that affect the development of the nematodes, and consequently the PWD symptoms, the recent findings as the identification of pine volatiles and the experiments on the tolerance to PWN [52] as well as the simulations on the spread of the nematode to focus the controlling efforts in regions with high susceptibility to the spread of this pest.

## 5 References

1. Internatioanal Standard for Phytosanitary Measures. Diagnostic protocols for regulated pests DP 10 : Bursaphelenchus xylophilus. in **ISPM 27**, DP 10-1-DP 10-36 (2016).

2. EPPO (European and Mediterranean Plant Protection Organization). Data sheets on Quarentine Pests - Bursaphelenchus xylophilus. in *Bulletin OEPP/EPPO Bulletin* (2004).

3. Vicente, C., Espada, M., Vieira, P. & Mota, M. Pine Wilt Disease: A threat to European forestry. *European Journal of Plant Pathology* **133**, 89–99 (2012).

4. Sousa, E., Vale, F. & Abrantes, I. *Pine Wilt Disease in Europe: Biological Interactions and Integrated Management*. (FIG - Indústrias Gráficas, SA, 2015).

5. European and Mediterranean Plant Protection Organization (EPPO). Bursaphelenchus xylophilus and its vectors: Procedures for official control. in *EPPO Bulletin* **42**, 477–485 (2012).

6. Naves, P., Bonifácio, L. & de Sousa, E. The pine wood nematode and its local vectors in the mediterranean basin. in *Insects and Diseases of Mediterranean Forest Systems* 329–378 (Springer International Publishing, 2016). doi:10.1007/978-3-319-24744-1_12

7. Naves, P. M., Sousa, E. & Rodrigues, J. M. *Biology of Monochamus galloprovincialis (Coleoptera, Cerambycidae) in the Pine Wilt Disease Affected Zone, Southern Portugal*. *Estação Florestal Nacional* **16**, (Silva Lusitana, Lisboa. Portugal, 2008).

8. Instituto da Conservação da Natureza e das Floretas (ICNF). IFN6 – Áreas dos usos do solo e das espécies florestais de Portugal continental em 1995, 2005 e 2010. in *6º Inventário Florestal Nacional* 34 (2013).

9. Branco, M., Bragança, H., Sousa, E. & Phillips, A. J. Pests and Diseases in Portuguese Forestry: Current and New Threats. in *Forest Context and Policies in Portugal* Chapter 5, 117-127 (Springer International Publishing, 2014). doi:10.1007/978-3-319-08455-8_5

10. Islam, M. S. Pinewood Nematode Bursaphelenchus xylophilus - Biology and Durable Control. *ResearchGate* (2015). doi:10.13140/RG.2.1.3040.7201

11. Yazaki, K. *et al. Pine wilt disease causes cavitation around the resin canals and irrecoverable xylem conduit dysfunction*. *Journal of Experimental Botany* **69**, (2018).

12. Ribeiro, B. *et al. Pine wilt disease: detection of the pinewood nematode (Bursaphelenchus xylophilus) as a tool for a pine breeding programme*. *Forest Pathology* **42**, 521–525 (2012).

13. Richards, O. W. & Davies, R. G. *IMMS' General Textbook of Entomology*. **61**, (Springer Netherlands, 1977).

14. Naves, P. M., De Sousa, E. M. & Quartau, J. A. Winter dormancy of the pine sawyer Monochamus galloprovincialis (Col., Cerambycidae) in Portugal. *J. Appl. Entomol.* **131**, 669–673 (2007).

15. Svacha, P. & Lawrence, J. F. *Handbook of Zoology Arthropoda: Insecta*. **3: Morphol**, (2014).

16. Rose, A. H. Some Notes on the Biology of Monochamus scutellatus (Say) (Coleoptera: Cerambycidae). *Can. Entomol.* **89**, 547–553 (1957).

17. Snodgrass, R. E. Respiratory system. in *Principles of Insect Morphology* 422–463 (McGraw-Hill Book Company, Inc., 1935).

18. Richards, O. W. & Davies, R. G. The Respiratory System. in *IMMS' General Textbook of Entomology* Volume I, 209-229 (Chapman and Hall Ltd., 1977).

19. Chapman, R. Gaseous exchange. *The Insects: Structure and Function* (eds. Simpson, S. J. & Douglas, A. E.) 501–528 (Cambridge University Press, 2013).

20. Richards, O. W. & Davies, R. G. Order 22 Coleoptera (Beetles). in *IMMS' General Textbook of Entomology* Volume II, 816-836, 892-895 (Chapman and Hall Ltd., 1977).

21. Socha, J. J. & De Carlo, F. Use of synchrotron tomography to image naturalistic anatomy in insects. in *Developments in X-Ray Tomography VI* **7078**, 70780A (2008).

22. Sombke, A., Lipke, E., Michalik, P., Uhl, G. & Harzsch, S. Potential and limitations of X-Ray micro-computed tomography in arthropod neuroanatomy: A methodological and comparative survey. *J. Comp. Neurol.* **523**, 1281–1295 (2015).

23. Wipfler, B., Pohl, H., Yavorskaya, M. I. & Beutel, R. G. A review of methods for analysing

insect structures — the role of morphology in the age of phylogenomics. *Current Opinion in Insect Science* **18**, 60–68 (2016).

24. Sena, G. *et al.* Phase contrast x-ray synchrotron microtomography for virtual dissection of the head of Rhodnius prolixus. in *Journal of Physics: Conference Series* **499**, (2014).

25. Baird, E. & Taylor, G. Quick guide X-ray micro comptuted-tomography. *Current Biology* **27**, R289–R291 (2017).

26. Alba-Tercedor, J. & Sáinz-Cantero Caparrós, C. E. Studying Aquatic Insects Anatomy with the SkyScan 1172 high-resolution micro-CT. in *SkyScan User Meeting 2010* 2: 8-11 (2010).

27. Iwan, D., Kamiński, M. J. & Raś, M. The Last Breath: A μCT-based method for investigating the tracheal system in Hexapoda. *Arthropod Struct. Dev.* **44**, 218–227 (2015).

28. Verdú, J. R., Alba-Tercedor, J. & Jiménez-Manrique, M. Evidence of different thermoregulatory mechanisms between two sympatric Scarabaeus species using infrared thermography and micro-computer tomography. *PLoS One* **7**, (2012).

29. Bentley, M. D., Ortiz, M. C., Ritman, E. L. & Carlos Romero, J. The use of microcomputed tomography to study microvasculature in small rodents. *Am. J. Physiol. - Regul. Integr. Comp. Physiol.* **282**, (2002).

30. Alba-Tercedor, J. A simple solution to help mounting centered samples to scan when using the Skyscan micro-CT attachment for SEM. 1–4 (2010).

31. Alba-Tercedor, J. & Sánchez-Tocino, L. The use of the SkyScan 1172 high-resolution micro-CT to elucidate if the spicules of the "sea slugs"(Mollusca: Nudibranchia, Opisthobranchia) have a structural or a defensive function. *MicroCT User Meet. Abstr. B.* 113–121 (2011).

32. Alba-Tercedor, J. & Sáinz-Cantero Caparrós, C. E. Volume rendering reconstructions of the anatomy of small aquatic beetles ( Insecta : Coleoptera ) scanned with the Skyscan 1172 high resolution a d b e f. *SkyScan Micro-CT Users Meet. 2012* 75–84 (2012).

33. Figueiredo, A. C., Barroso, J. M. G., Pedro, L. M. G. & Oliveira, M. M. M. G. de. *Guia Prático de Biologia Celular*. (Associação dos Estudantes da Faculdade de Ciências de Lisboa, 2003).

34. Zhou, W., Apkarian, R., Wang, Z. L. & Joy, D. Fundamentals of scanning electron microscopy (SEM). in *Scanning Microscopy for Nanotechnology: Techniques and Applications* 1–40 (Springer New York, 2007). doi:10.1007/978-0-387-39620-0_1

35. Douglas F, B. *Critical Point Drying of Biological Specimens for Scanning Electron Microscopy*. (2014). doi:10.1385/1-59259-030-6

36. Supercritical fluids - Supercritical fluids. Available at: http://www.supercriticalfluid.org/Supercritical-fluids.146.0.html. (Accessed: 21st January 2020)

37. Bisht, D. & Iqbal, Z. Lyophilization - Process and optimization for Pharmaceuticals. *Int. J. Drug Regul. Aff.* **3**, 30–40 (2018).

38. Adsorption, Absorption and Desorption - What's the Difference? Chromatography Today. Available at: https://www.chromatographytoday.com/news/hplc-uhplc/31/breaking-news/adsorption-absorption-and-desorption-what39s-the-difference/31397. (Accessed: 15th January 2020)

39. What is lyophilization? How does it work? Millrock Technology, Inc. Available at: https://www.millrocktech.com/lyosight/lyobrary/what-is-lyophilization/. (Accessed: 17th January 2020)

40. Eaton, P. *et al.* A direct comparison of experimental methods to measure dimensions of synthetic nanoparticles. *Ultramicroscopy* **182**, 179–190 (2017).

41. Reis, F. J. J. dos, de Barros e Silva, V., de Lucena, R. N., Mendes Cardoso, B. A. & Nogueira, L. C. Measuring the Pain Area: An Intra- and Inter-Rater Reliability Study Using Image Analysis Software. *Pain Practice* **16**, 24–30 (2016).

42. ImageJ User Guide - IJ 1.46r | Overlays. Available at: https://imagej.nih.gov/ij/docs/guide/146-11.html. (Accessed: 9th September 2019)

43. Figueiredo, A. C. & Pais, M. S. S. Ultrastructural Aspects of the Glandular Cells from the Secretory Trichomes and from the Cell Suspension Cultures of Achillea millefolium L. ssp. millefolium. *Annals of Botany* **74**, 179–190 (1994).

44. Alba-Alejandre, I., Alba-Tercedor, J. & Vega, F. E. Micro-CT to Document the Coffee Bean Weevil, Araecerus fasciculatus (Coleoptera: Anthribidae), Inside Field-Collected Coffee Berries (Coffea canephora). *Insects* **9**, 1–9 (2018).

45. Iwan, D., Jan Kaminski, M. & Rás, M. The Last Breath: A CT-based method for investigating the tracheal system in Hexapoda. *Arthropod Structure & Development* **44**, 218–227 (2015).

46. BRUKER. CT-Analyser User Guide. in *Manual for Bruker-microCT CT-Analyser v. 1.13* 1–139 (2013). Available at: https://pt.scribd.com/document/399938250/CTan-UserManual

47. Bruker Skyscan. Bruker-MicroCT method note (CTAn): externally edited image format ROI. Available at: https://www.bruker.com/products/microtomography/academy/academy.html

48. Faria, J. M. S., Sena, I., Maleita, C., Vieira da Silva, I., Ascensão, L., Abrantes, I., Bennett, R. N., Mota, M., Figueiredo, A. C. In vitro co-culture of Solanum tuberosum hairy roots with Meloidogyne chitwoodi: Structure, growth and production of volatiles. *Plant Cell, Tissue and Organ Culture* **118**, 519–530 (2014).

49. Bonifácio, L. Impacte e evolução da doença da murchidão dos pinheiros (Pine Wilt Disease), na zona afetada a sul do rio Tejo. (Faculdade de Ciências, Universidade de Lisboa, 2009).

50. Helm, B. R. *et al.* Micro-computed tomography of pupal metamorphosis in the solitary bee Megachile rotundata. *Arthropod Structure & Development* **47**, 521–528 (2018).

51. Pereira, M. F. C., Maurício, A. M. & Leal, A. C. Insect microstructure. Oral comunication at *Interactions behind the Pine Wilt Disease Seminar,* INIAV, Oeiras (2018).

52. Menéndez-Gutiérrez, M., Alonso, M., Toval, G. & Díaz, R. Testing of selected Pinus pinaster half-sib families for tolerance to pinewood nematode (Bursaphelenchus xylophilus). *For. An Int. J. For. Res.* **91**, 38–48 (2018).

53. Pogonocherus perroudi perroudi. Available at: http://www.cerambyx.uochb.cz/pogonocherus_perroudi_perroudi.php. (Accessed: 1st October 2018)

54. Acanthocinus griseus. Available at: http://www.cerambyx.uochb.cz/acanthocinus_griseus.php. (Accessed: 1st October 2018)

55. Arhopalus syriacus. Available at: http://www.cerambyx.uochb.cz/arhopalus_syriacus.php. (Accessed: 16th November 2019)

56. Monochamus galloprovincialis pistor. Available at: http://www.cerambyx.uochb.cz/monochamus_galloprovincialis_pistor.php. (Accessed: 1st October 2018)

## 6 Appendices

**Appendix I –** Information on anatomic and ecologic features of the studied species [iii].

| Species | M. galloprovincialis | A. syriacus | A. griseus | P. perroudi |
|---|---|---|---|---|
| **Sub-family** | Lamiinae | Spondylidinae | Lamiinae | Lamiinae |
| **Body length** | 12 – 26 mm | 12 – 23 mm | 8 – 13 mm | 4 – 8 mm |
| **Life cycle** | 1 year | 2-3 years | 1-2 years | 1-2 years |
| **Emergence** | May - September | May – August | April – August | April – August |
| **Host plant** | Pines (Pinus spp) | Pinus spp, rarely spruce (Picea) | Mainly coniferous trees (Pinus, Picea, Abies), reported from oak (Quercus) | Pine's dying branches |
| **Geographic Distribution** | Central, West and North Europe, Russia, Turkey, Ukraine | Mediterranean region, Canary Islands | Europe, Russia, Asia | Mediterranean region |
| **Sexual dimorphism** | Yes, visible in antennae colouration and lenght | Not present | Yes, females have an evident ovipositor organ | Not present |
| **Larval phase** | Under the bark of host trees | | | Under the bark of dying trees |
| **Adult phase** | New sprouts of the crown of host trees | On the host tree bark during the night or in bark crevices during the day | No information found | Dying branches of the host tree |

[iii] Information collected from http://www.cerambyx.uochb.cz/index.php [53–56] and from Sousa, E., Vale, F. & Abrantes, I. *Pine Wilt Disease in Europe: Biological Interactions and Integrated Management*. (FIG - Indústrias Gráficas, SA, 2015) [4].

**Appendix II –** Parameters setting for Micro-CT acquisitions.

The species are *M. galloprovincialis* (Mg), *A. syriacus* (As), *A. grisues* (Ag) and *P. perroudi* (Pp), 'M' is for Male specimens and 'F' for female.

| Specimen | Treatment | Pixel size (µm) | Rotation (degrees) | Source voltage (kV) | Source current (uA) | Frame averaging | Duration |
|---|---|---|---|---|---|---|---|
| Ag000 (F) | no | 3.44 | 0.5 | 59 | 167 | 3 | 7h30 |
| Ag002 (M) | no | 3.62 | 0.5 | 40 | 250 | 3 | 7h |
| As0030 | Lyophilized | 4.16 | 0.350 | 40 | 250 | 3 | 11h15 |
| MgP 0011 | GA+CPD | 3.78 | 0.3 | 79 | 125 | 3 | 18h |
| Mg (M) | GA+CPD | 3.80 | 0.3 | 37 | 234 | 3 | 19h |
| Mg (F) | GA+CPD | 3.44 | 0.250 | 59 | 167 | 3 | 21h |
| Ag 001 | no | 3.08 | 0.250 | 79 | 125 | 3 | 14h |
| MgP 000 | no | 3.62 | 0.350 | 59 | 167 | 3 | 6h |

**Appendix III –** Registration of the specimens sent to SEM.

In the column "Measured" the specimens with no information are the ones that have not been imaged, the treatment "GA+CP" stand for the chemical fixation, (GA – Glutaraldehyde, CP - Critical Point Dried), Elytra length (in millimeter) is a standard measure in Entomology, it was always carried out in the right elytra, the species are *M. galloprovincialis* (Mg), *A. syriacus* (As), *A. grisues* (Ag) and *P. perroudi* (Pp), 'M' is for Male specimens and 'F' for female.

| Species | | ID | Treatment | Elytra length (mm) | Measured |
|---|---|---|---|---|---|
| Mg | adult M | Mg 001 | no | 12.722 | Yes |
| | adult M | Mg 002 | no | 11.718 | Yes |
| | adult F | Mg 003 | no | 11.714 | Yes |
| | adult F | Mg 004 | no | 11.443 | Yes |
| | adult F | Mg 005 | no | 12.989 | Yes |
| | Pupa | Mg P 001 | no | | Yes |
| | adult M | Mg 0002 | GA+CPD | 10.787 | |
| | adult F | Mg 0007 | GA+CPD | 16.091 | |
| | adult M | Mg 0011 | GA+CPD | 9.862 | |
| | adult F | Mg 0013 | GA+CPD | 13.595 | |
| | adult M | Mg 0014 | GA+CPD | 11.267 | |
| | adult F | Mg 0015 | GA+CPD | 11.540 | |
| | adult M | Mg 0017 | GA+CPD | 10.733 | |
| | adult M | Mg 0018 | GA+CPD | 11.318 | |
| | adult F | Mg 0019 | GA+CPD | 11.373 | |
| | adult M | Mg 0031 | Lyophilized | 13.212 | |
| | adult M | Mg 0032 | Lyophilized | 11.247 | Yes |
| | adult F | Mg 0033 | Lyophilized | 13.742 | Yes |
| | adult F | Mg 0034 | Lyophilized | 12.863 | Yes |
| | adult F | Mg 0035 | Lyophilized | 11.933 | Yes |
| | Pupa | Mg P 0000 | GA+CPD | | |
| | Pupa | Mg P 0003 | GA+CPD | | |
| | Pupa | Mg P 0005 | GA+CPD | | |
| | Pupa | Mg P 0006 | GA+CPD | | |
| | Pupa | Mg P 0007 | GA+CPD | | |
| | Pupa | Mg P 0009 | GA+CPD | | |
| | Pupa | Mg P 0010 | GA+CPD | | |
| | Pupa | Mg P 0012 | GA+CPD | | |
| | Pupa | Mg P 0014 | GA+CPD | | |
| | Pupa | Mg P 0015 | GA+CPD | | |
| | Pupa | Mg P 0016 | GA+CPD | | |
| | Pupa | Mg P 0017 | GA+CPD | | |
| | Pupa | Mg P 0019 | GA+CPD | | |
| | Pupa | Mg P 0020 | GA+CPD | | |
| As | Adult | As 001 | No | 9.671 | Yes |
| | Adult | As 0002 | GA+CPD | 10.118 | Yes |
| | Adult | As 0004 | GA+CPD | 10.742 | Yes |

| | | | | | |
|---|---|---|---|---|---|
| | Adult | As 0005 | GA+CPD | 10.575 | Yes |
| | Adult | As 0030 | Lyophilized | 14.953 | Yes |
| | Adult | As 0032 | Lyophilized | 9.382 | Yes |
| | Adult | As 0033 | Lyophilized | 9.911 | No |
| | Adult | As 0034 | Lyophilized | 8.177 | Yes |
| | Adult | As 0035 | Lyophilized | 8.957 | Yes |
| **As** | Adult | As 0036 | Lyophilized | 9.028 | Yes |
| | adult | As 0037 | Lyophilized | 8.671 | Yes |
| | Pupa | As P 0002 | GA+CPD | | No |
| | Pupa | As P 0003 | GA+CPD | | Yes |
| | Pupa | As P 0004 | GA+CPD | | Yes |
| | Pupa | As P 0005 | GA+CPD | | |
| | adult F | Ag 001 | No | 8.462 | No |
| **Ag** | adult F | Ag 002 | No | 9.434 | Yes |
| | adult F | Ag 0030 | Lyophilized | 8.432 | Yes |
| | adult M | Ag 0032 | Lyophilized | 8.838 | Yes |
| **Pp** | adult | Pp 001 | No | 5.012 | Yes |

# 7 Annex

**Annex I** - Survey of insects emerging from dead pine trees infested with B. xylophilus, in Portugaliv.

| Order/ Family/ Species | Number of individuals sampled (n) | B. xylophilus presence (+) / absence (-) |
|---|---|---|
| Coleoptera | | |
| Cerambycidae | | |
| *M. galloprovincialis* | 1.680 | + |
| *Arhopalus ferus* | 95 | - |
| *A. syriacus* | 80 | - |
| *Pogonocherus perroudi* | 55 | - |
| *Acanthocinus griseus* | 83 | - |
| *Spondylis buprestoides* | 22 | - |
| *Rhagium inquisitor* | 3 | - |
| *Ergates faber* | 3 | - |
| Scolytinae | | |
| *Orthotomicus erosus* | 899 | - |
| *Tomicus piniperda* | 168 | - |
| *Ips sexdentatus* | 300 | - |
| *Hylurgus ligniperda* | 557 | - |
| *Pityogenes* sp. | 175 | - |
| *Hylastes* sp. | 34 | - |
| Buprestidae | | |
| *Chrysobothris solieri* | 50 | - |
| *Calcophora mariana* | 11 | - |
| *Phaenops cyanea* | 3 | - |
| Curculionidae | | |
| *Pissodes castaneus* | 185 | - |
| *Eremotes porcatus* | 50 | - |
| *Hylobius* sp, | 62 | - |
| Elateridae | | |
| Unidentified sp. | 10 | - |
| Hymenoptera | | |
| Siricidae | | |
| *Sirex noctilio* | 3 | - |
| Total | 4.528 | |

---

iv data from Sousa, E., Vale, F. & Abrantes, I. *Pine Wilt Disease in Europe: Biological Interactions and Integrated Management*. (FIG - Indústrias Gráficas, SA, 2015) [4]

**Annex II** – Images of the studied species [v].



*Figure 7.4: Adult, male and female, Monochamus galloprovincialis (Photo © M.Hoskovec).*
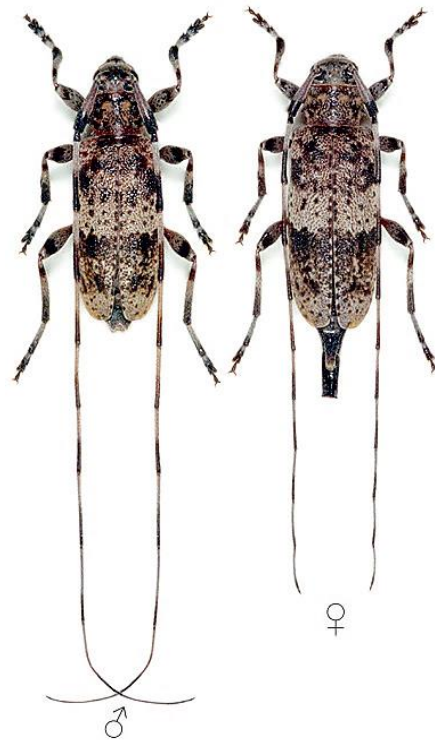


*Figure 7.3: Adult, male and female, Acanthocinus griseus (Photo © M.Hoskovec)*



*Figure 7.1: Adult Pogonocherus perroudi (Photo © M.Hoskovec)*



*Figure 7.2: Adult Arhopalus syriacus (Photo © M.Hoskovec)*

---

[v] The images do not represent the real size, complement with the features from Appendix I. Photographs from http://www.cerambyx.uochb.cz/index.php [53–56].